Membrane Tension Accelerates Rate-limiting Voltage-dependent Activation and Slow Inactivation Steps in a Shaker Channel

Ulrike Laitko and Catherine E. Morris

Ottawa Health Research Institute Ottawa, Ontario, Canada K1Y 4E9

ABSTRACT A classical voltage-sensitive channel is tension sensitive—the kinetics of Shaker and S3–S4 linker deletion mutants change with membrane stretch (Tabarean, I.V., and C.E. Morris. 2002. *Biophys. J.* 82:2982–2994.). Does stretch distort the channel protein, producing novel channel states, or, more interestingly, are existing transitions inherently tension sensitive? We examined stretch and voltage dependence of mutant 5aa, whose ultra-simple activation (Gonzalez, C., E. Rosenman, F. Bezanilla, O. Alvarez, and R. Latorre. 2000. *J. Gen. Physiol.* 115:193–208.) and temporally matched activation and slow inactivation were ideal for these studies. We focused on macroscopic patch current parameters related to elementary channel transitions: maximum slope and delay of current rise, and time constant of current decline. Stretch altered the magnitude of these parameters, but not, or minimally, their voltage dependence. Maximum slope and delay versus voltage with and without stretch as well as current rising phases were well described by expressions derived for an irreversible four-step activation model, indicating there is no separate stretch-activated opening pathway. This model, with slow inactivation added, explains most of our data. From this we infer that the voltage-dependent activation path is inherently stretch sensitive. Simulated currents for schemes with additional activation steps were compared against datasets; this showed that generally, additional complexity was not called for. Because the voltage sensitivities of activation and inactivation differ, it was not possible to substitute depolarization for stretch so as to produce the same overall P_O time course. What we found, however, was that at a given voltage, stretch-accelerated current rise and decline almost identically—normalized current traces with and without stretch could be matched by a rescaling of time. Rate-limitation of the current falling phase by activation was ruled out. We hypothesize, therefore, that stretch-induced bilayer decompression facilitates an in-plane expansion of the protein in both activation and inactivation. Dynamic structural models of this class of channels will need to take into account the inherent mechanosensitivity of voltage-dependent gating.

KEY WORDS: mechanosensitive • 5aa linker mutant • voltage-gated • stretch • S3–S4

The Journal of General Physiology

INTRODUCTION

Mechanosensitivity in Ion Channels

Mechanical forces change the open probability (P_O) of many ion channels. Prokaryotic osmotic valve channels (MscL, MscS) respond to near-lytic bilayer tension (Blount, 2003). In eukaryotes, mechanosensitive channels that transduce touch, sound, and gravity are thought to link to filamentous proteins that transmit mechanical gating energy. Curiously, these mechanotransducer specialists show no evidence of susceptibility to mild bilayer tension excursions (e.g., Goodman and Schwarz, 2003), whereas such susceptibility is reasonably common among eukaryotic channels not seen principally as mechanotransducers.

Among voltage-gated channels, mechanosusceptibility has diverse manifestations. An irreversible shift to fast gating occurs with stretch for Na channel α subunits (Shcherbatko et al., 1999; Tabarean et al., 1999). Na channel mechanosensitivity in smooth muscle may have physiological and pathophysiological consequences (Ou et al., 2003). Stretch reversibly increases L-type (Langton, 1993) and N-type calcium currents without altering the speed of activation (Calabrese et al., 2002). Apparent mechanosensitivity has been noted for native voltage-gated K channels (Fig. 2 of Pahapill and Schlichter, 1992; Schoenmakers et al., 1995). Increased activity with stretch in Ca-activated maxi-K channels (Taniguchi and Guggino, 1989; Mienville et al., 1996) may be mediated by fatty acids (Ordway et al., 1995) and/or channel subdomains (Naruse et al., 2003). Of particular interest is the prototypical voltage-gated K channel, Shaker, where membrane stretch robustly affects the extent of voltage-dependent activation (Gu et al., 2001; Tabarean and Morris, 2002).

Insofar as bilayers are elastic springs coupled to embedded channels, increased membrane tension will increase the rate of transitions into larger-area channel conformations. Further, bilayers under tension become thin, so hydrophobic mismatch effects at lipid–protein

Address correspondence to: Catherine E. Morris, Neuroscience, Ottawa Health Research Institute, Ottawa Hospital, 725 Parkdale Ave., Ottawa, Ontario, Canada K1Y 4E9. Fax: (613) 761-5330; email: cmorris@ohri.ca

Abbreviation used in this paper: LS, linear substraction.

interfaces may occur. Internal tension in a protein could influence conformational energies in many ways, so we require from Shaker a more detailed description of how elevated tension affects activation kinetics. In particular we seek to distinguish between two possibilities: (a) a separate activation pathway, a "mechanical gate" or mechanosensor motif, uses the energy of membrane tension to open the channel, and (b) Shaker is susceptible to stretch because voltage sensing is inherently sensitive to membrane tension.

Shaker Channel Activation

The activation of voltage-gated channels originates in movement of the voltage sensor—the part of the channel that senses and transduces changes in the transmembrane electric field. Shaker is a homotetramer whose subunits have six transmembrane segments, S1–S6, with S4 containing a periodic succession of positively charged amino acids that are major contributors to the gating charge movement (Aggarwal and MacKinnon, 1996; Seoh et al., 1996). During depolarization, some of these residues change their exposure from intracellular to extracellular (Larsson et al., 1996; Yusaf et al., 1996). S4 is thus seen as the crucial part of the voltage sensor.

During activation and deactivation, charged residues in S4 move, so the voltage sensor is a specialized dielectric in the membrane electric field. Energies of the resting and active subunit conformations, and thereby the probability of channel activation, change with voltage; depolarization favors activation. Models have S4 moving in an irregularly shaped aqueous "gating canal" formed by other parts of the protein. S4 rotation is envisaged (Cha et al., 1999; Glauner et al., 1999), with parts of S4 facing water-accessible vestibuli that penetrate the channel protein and define the region of steepest electrical potential gradient. In one hypothesis (Gonzalez et al., 2001; Bezanilla, 2002), a tilted S4 performs a rigid ~180° rotation that switches exposure of the positive charges from the intra- to the extracellular side. In another (Gandhi and Isacoff, 2002), this rotation is embedded in a helical screw motion that moves S4 relative to neighboring segments.

A recent crystal structure for the Shaker-related bacterial KvAP channel (Jiang et al., 2003a) challenges these views. It suggests S4 and part of S3 form a helix-turn-helix "voltage sensor paddle" at the perimeter of the channel, with depolarization making paddles move through lipid from more horizontal to more vertical positions (Jiang et al., 2003b). While radically different, this would make it no less likely that bilayer properties—tension, length, and flexibility of the lipid tails—would influence channel gating. We note, however, that marked slowing of activation by deletion of the S3–S4 linker (Gonzalez et al., 2000) makes good sense in models based on S4 movement relative to S3, but is counterintuitive for the paddle model, where S3 and S4 move together and should experience less resistance to movement after deletion of ~25 residues at what would be the paddle's tip. In any event, new studies (Broomand et al., 2003; Gandhi et al., 2003) indicate that the paddle model does not apply for Shaker.

Although physiological terminology has S4 "resting" at hyperpolarized voltages and "active" at depolarized voltages, absence of an electrical field causes S4s to collapse to their "active" state. Since native channels prefer being open at 0 mV, it might also be expected that "open" is the default state for Shaker's pore and gate region (S5s and S6s), but an energetics analysis of gating for pore mutants (Yifrach and MacKinnon, 2002) shows that the pore is at its lowest energy when closed. Thus, during activation the voltage sensors must overcome the intrinsically favored closed pore conformation, presumably by applying a lateral force that bends the S6 gating hinges, forcing the crossed inner helix bundle of S5 and S6 (Yellen, 2002) to splay apart.

Shaker Channel Inactivation

Native Shaker channels have complex inactivation. There is fast N-type (Hoshi et al., 1990), and two kinds of slow inactivation. The latter, C-type (Olcese et al., 1997) and P-type (Loots and Isacoff, 2000) inactivation, yield low conductivity channels with dramatically reduced K^+ selectivity (Starkus et al., 1997). In contrast to deactivated channels, inactivated channels are not directly susceptible to new activation. N-type inactivation involves structures absent in the truncated channels used here (the NH_2-terminally truncated wild-type will henceforth be alluded to as WT). In WT, C-type inactivation (which persists in the truncated channels) is markedly slower than activation. By contrast, for certain S3–S4 linker deletants, including the one used here, current rise and decline happen on similar time scales (Tabarean and Morris, 2002) and so can be studied simultaneously.

S3–S4 Linker Mutants

One approach to investigating S4 motions in Shaker activation has been deletion of the extracellular S3–S4 linker, a maneuver designed to reduce the freedom of S4 to move with respect to the transmembrane electric field. Gonzalez et al. (2000) defined this linker as residues 330–360, and found substantially slower activation with the linker reduced to 10, 5, or 0 amino acids (mutants "10aa", "5aa", and "0aa"). Also, activation was shifted toward more depolarized voltages.

In spite of sluggish responses to voltage steps, the S3–S4 linker mutants are mechanosensitive and, importantly, require no more mechanical energy than WT for comparable P_O changes (Tabarean and Morris, 2002).

This suggests that voltage-dependent activation in Shaker is inherently sensitive to bilayer stretch. A useful aspect of activation kinetics in S3–S4 linker mutants has been noted (Gonzalez et al., 2000)—unlike WT, 5aa conductance versus voltage (g(V)) relations are well fitted by fourth-order Gaussians, hinting that the 5aa tetramer has one rate-limiting activation step per subunit. Such simplicity, plus the similar time scales of activation and inactivation make 5aa particularly desirable for a kinetic study of Shaker mechanosensitivity by providing more (and more easily interpreted) kinetic information. Using 5aa we were able to ask if increased membrane tension affects the voltage-sensing and -inactivation steps themselves or if it modulates the channel in previously unknown ways.

MATERIALS AND METHODS

Constructs, Expression

Channels were expressed in *Xenopus* oocytes. Oocytes were defolliculated with collagenase (2 mg/ml in Ca-free OR2 medium), ripe oocytes selected and injected with the 5–25 ng 5aa cRNA, provided by Dr. R. Latorre. 5aa is the ShakerH4Δ-Δ(330–355) mutant (Gonzalez et al., 2000) that differs from the NH_2-terminally truncated Shaker version ShakerH4 Δ(6–46) that we refer to as WT (Gu et al., 2001) by deletion of 25 of the 30 S3/S4 linker residues. Injected oocytes were maintained at 18°C in OR2 solution supplemented with 50 units penicillin, 50 μg streptomycin, and 0.125 μg amphotericin B (antibiotic/antimycotic from GIBCO/BRL).

Electrophysiological Recordings

The vitelline layer was removed manually after shrinking the oocytes in hyperosmolar solution. Up to three cell-attached patch clamp recordings were made per oocyte. Pipettes (∼3–6 MΩ) were pulled from borosilicate (Garner; 1.15 mm inner diameter, OD 1.65) using a L/M-3P-A (List Medical). Currents, filtered at 2 kHz, were recorded using an Axopatch 200B (Axon Instruments, Inc.) amplifier and digitized using pClamp6 (Axon Instruments, Inc.) software and A/D converter Digidata 1200 (Axon Instruments, Inc.). Currents were corrected for linear capacitive currents with the amplifier's compensation circuits, residual capacitive and leakage currents were usually corrected by linear subtraction.

As 5aa has slow kinetics, performing the time-consuming P/N (see pClamp; Axon Instruments, Inc.) linear subtraction (LS) procedure for every trial would limit the number of trials per patch and, for stretch runs, subject patches to long destabilizing periods of suction. Instead, we mostly opted for a more economical LS method: for each patch six responses to a step from −90 to −60 mV were averaged at the start of recording and also whenever the amplifier gain was changed. During analysis, this averaged LS trace was upscaled appropriately and subtracted from currents from that patch. Nevertheless, leak sometimes changes over time and capacitive transients are sometimes not entirely linear in voltage. Changes in leak were directly obvious from inspection of the base line currents, and data with such shifts were rejected. What of the capacitive transients? In Fig. 1 A, traces with and without P/4 LS are overlayed. In each panel the faster currents are with stretch, the slower ones, without (−45 mm Hg used for stretch). Unlike the minimal leak currents, capacitive transients without LS are large, though quite well separated from the channel currents (a benefit of 5aa over WT). As illustrated, however, even for a step from −90 to 90 mV, uncompensated capacitive currents minimally obstruct the channel currents during activation. Since even forgoing LS was not problematic, we are confident that the small capacitive transients remaining after using our LS procedure did not affect the kinetic analysis.

The patch pipette solution contained (in mM) 95 NaCl, 1 KCl, 5 $MgCl_2$, and 5 HEPES at pH 7.2; the bath solution contained (in mM) 100 K-Aspartate, 20 KCl, and 2 EGTA at pH 7.2. To inhibit stretch-activated endogenous cation channels 10–20 μM gadolinium was sometimes included in the pipette (Yang and Sachs, 1989). Gadolinium has been reported to right-shift the Shaker g(V) relation by 10–20 mV (Gu et al., 2001; Tabarean and Morris, 2002). The experiments were performed at room temperature.

Tension

Membrane patches were stretched by suction (negative pressure) applied via the patch pipette sideport. Suction was created with a syringe (a manual valve was opened to reset to atmospheric pressure) and measured with a pneumatic transducer pressure tester (DPM-1B; Bio-Tek). Positive pressure is not as practical because of poor seal stability, but we convinced ourselves that it had entirely comparable effects on currents. Suction is an effective way to reversibly stretch membrane patches. However, tip diameter (and hence patch size and curvature) and mechanical properties of membranes differ among patches and without imaging the patch, one cannot quantify membrane tension.

We adopted two different experimental protocols: "families" and "before, during, after". For families, the voltage was stepped from the holding potential (−90 mV) to increasingly depolarized levels, either with or without stretch. For "before, during, after", one or two measurements without stretch were followed by (usually) one measurement with stretch and then another without, repeated for as many test voltages as possible. In all protocols, pauses (>1 min) at −90 mV between voltage steps allowed for recovery from inactivation. We found that the voltage dependence of fits to kinetic parameters was usually smoother for "families" data.

Repeated stretching sometimes increased nonstretched current amplitudes, and in some cases also altered their kinetics. Such datasets were discarded; there may have been residual tension in some patches, while in others patch area might have increased, or oocyte membrane properties altered (see Tabarean et al., 1999).

Kinetic Analysis—5aa Activation

The opening of Shaker involves one or more preopening steps per subunit, plus one or more final concerted transition(s) (Hoshi et al., 1994; Zagotta et al., 1994a,b; Schoppa and Sigworth 1998a,b,c; Smith-Maxwell et al., 1998). Cooperativity between the voltage sensors has not been excluded but is not generally included in activation models.

As a kinetic signature of 5aa with and without stretch, we used the voltage dependence of the maximum slope and delay of macroscopic currents. This approach is similar to one described by Schoppa and Sigworth (1998a) who fitted exponentials to the late rising phase of WT currents, yielding an activation time constant and a characteristic delay. With 5aa, however, inactivation may corrupt the later rising phase, diminishing the maximum amplitude of the 5aa currents. Thus, the tangent to the current at the point of maximum slope (reached relatively early in the rising phase) was better for capturing the properties of 5aa activation, especially as a formula for this tangent can be straightforwardly derived for many activation models, a bonus for analysis. Fig. 1 B illustrates a by-eye determination of the maximum slope. This approach was used because, given the noise in the signal, determining a maximum slope from the maximum of the cur-

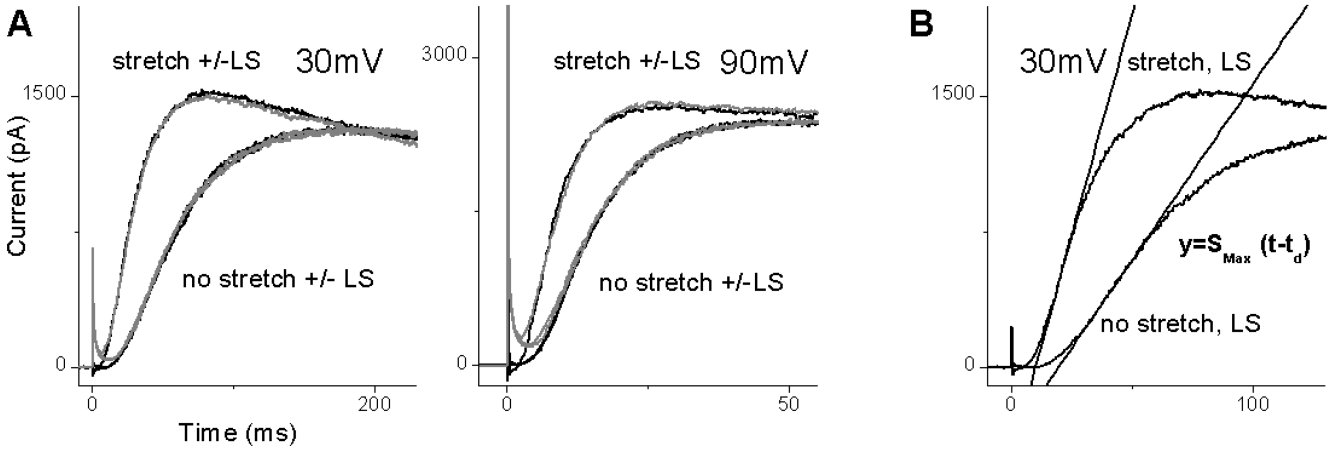

FIGURE 1. (A) Effect of linear subtraction (LS). 5aa currents during depolarizations from −90 mV to 30 and 90 mV with (black) and without (gray) linear subtraction are compared as described in the text. The faster currents in each panel were recorded with stretch (using −45 mm Hg), the slower currents before and after stretch. Channel currents and capacitive transients are well separated. The traces demonstrate that nonleaky patches were used and that 5aa, with its slow activation, was an ideal mutant for the kinetic analysis undertaken here. Thus, although LS was used routinely (see MATERIALS AND METHODS), it was not critical for obtaining accurate 5aa channel current amplitudes or maximum rates of rise. (B) Maximum slope line analysis. Maximum slope lines fitted to 30 mV leak-subtracted currents with/without stretch from A. The fit quantifies characteristic properties of current activation: S_{Max} − maximum slope, and t_d − delay.

rent derivative was not practical. Filtering and parameterizing the current then calculating a derivative would be no more precise than our method.

The slope and time axis intersection of the maximum slope line define two parameters (maximum slope and delay of the current) that are practical and reproducible, albeit in the case of delay somewhat arbitrary. Given a suitable activation model, they provide information about underlying (microscopic) properties of channel activation. The delay is a particularly valuable indicator of channel kinetics since (unlike slope) it withstands scaling of the current, and is thus independent of changes in driving force (reversal potential) or channel number that might arise in the course of prolonged experiments. Delays can be compared between patches, and kinetic information derived makes no assumptions about driving force.

Kinetic Analysis—5aa Inactivation

In 5aa, unlike WT, characteristic current rise and decline times are comparable, with currents declining to a plateau of small, but generally nonzero amplitude. The falling phase of the recorded currents was easily and consistently fit by the sum of one constant (the plateau current I_1) and one exponentially declining component,

$$I(t) = I_1 + I_0 e^{-t/\tau}, \quad (1)$$

although the plateau may in fact be a much more slowly declining component.

Data analysis was performed with Origin 6.0 (Microcal Software Inc.) and Maple 8 (Waterloo Maple Inc.) was used for simulations and calculations.

RESULTS

General

Membrane stretch is known to left-shift the P_O of Shaker WT and the 0aa, 5aa, and 10aa linker (Tabarean and Morris, 2002). For a cell-attached patch tested over an 80-mV range with 20 μM Gd^{3+} in the pipette, Fig. 2 A illustrates how stretch (−45 mmHg suction) affected 5aa currents. At −40 mV, which is well below the foot of the 5aa g(V) relation (see Gonzalez et al., 2000), and recall that Gd^{3+} right-shifts the g(V), there was no detectable channel current before or after stretch. With stretch this patch showed current noise, presumably due to rare 5aa channel activation plus imperfect blockade of endogenous mechanosensitive cation channels (the latter evidenced by stretch-induced noise in the holding current). At −20 mV without stretch, 5aa current was negligible, but with stretch the voltage step elicited a substantial outward current. At 0 and 40 mV, stretch accelerated current time courses and increased their amplitude. Effects of stretch on current amplitude were progressively less dramatic as P_O saturated at large depolarizations, but accelerated rising and falling phase kinetics remained evident. Fig. 2 B shows another patch below the foot of g(V); −40 mV elicited no current with or without stretch but stepping to −20 mV with stretch elicited time-dependent 5aa current (note the longer time base than in Fig. 2 A). Traces like Fig. 2 B make it qualitatively clear that stretch augmented 5aa activation, but larger depolarizations were used subsequently so 5aa kinetics with/without stretch could be compared quantitatively.

The stretch-induced outward currents were not due to the endogenous nonselective mechanosensitive cation conductance for the following reasons. (a) 20 μM Gd^{3+} almost completely blocked those channels. (b) Even without Gd^{3+}, they contributed only a few pA. (c)

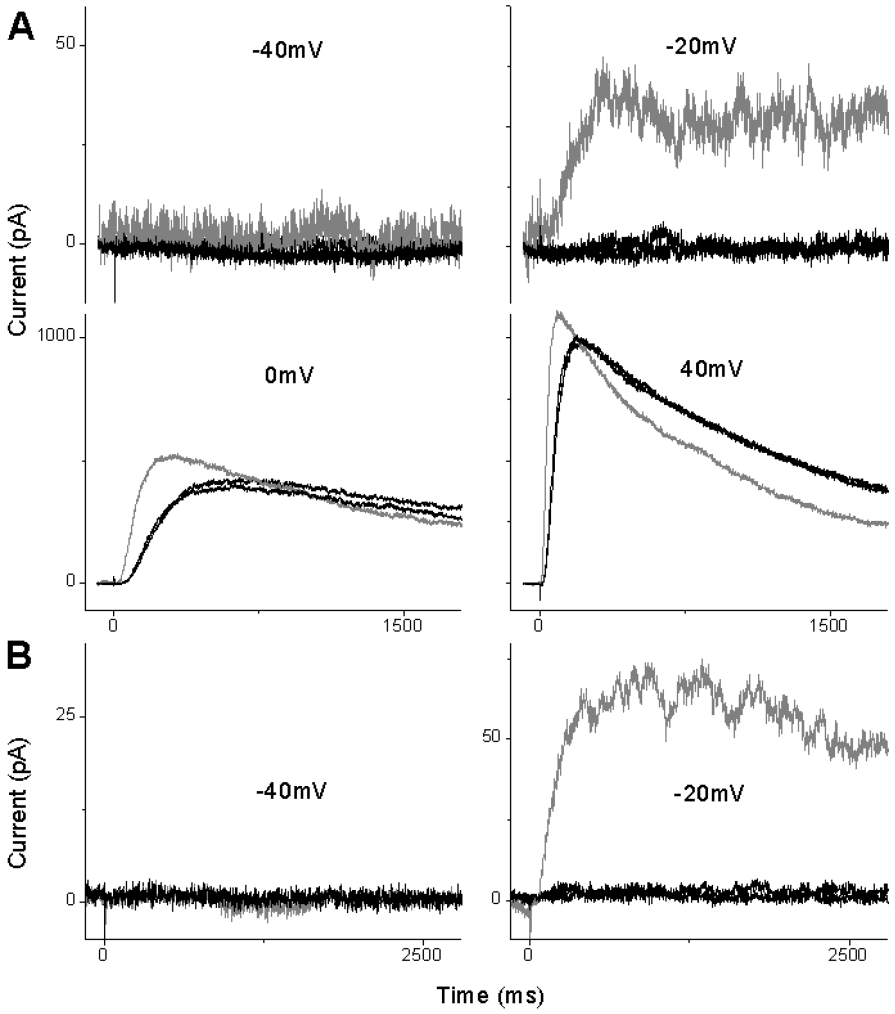

FIGURE 2. The effect of stretch on 5aa currents elicited by a depolarizing step from −90 mV. Gray, current with stretch (−45 mm Hg suction); black, current without stretch (before and after). 20 μM Gd^{3+} in pipette. The most dramatic stretch effect for Shaker channels, including 5aa, occurs at the foot of the g(V), where stretch enables a voltage step to elicit current where there had been none without stretch. In these two examples (A and B; different patches), −40 mV was just at (A) or below (B) the threshold for this effect, whereas −20 mV was above it. Macroscopic currents were absent without stretch, but at −20 mV with stretch a large time-dependent current developed. At larger depolarizations (0 and 40 mV in A), stretch accelerated both current rise and decline.

The endogenous currents reverse at ∼0 mV under our recording conditions, so the stretch effects e.g., at −20 mV, where endogenous and Shaker currents have different polarity, and at 0 mV, where endogenous currents vanish, can only be due to the heterologous K channels.

Two general ways whereby stretch might accelerate activation are: (a) stretch-induced deformation in some region of the channel might increase the probability of pore opening, independent of S4 movement. In this scenario, channels should open with stretch even at deeply hyperpolarized voltages. (b) Stretch could affect the rates of (some of) the conformational changes that occur during normal voltage-gating. However, as Fig. 2 illustrates, a particular suction stimulus could generate dramatic current response at −20 mV, but none at −40 mV, and since this alone argues strongly against hypothesis (a), we approach this study with a certain bias in favor of hypothesis (b).

To start, we asked a simple question motivated by the fact that moderate stretch has essentially the same effect on WT current amplitude and time course as applying several millivolts of additional depolarization (Tabarean and Morris, 2002). Are gating energies from stretch and depolarization completely interchangeable in Shaker channels? To test this exhaustively, a mutant like 5aa with a balanced, bipartite kinetic signature (i.e., activation and inactivation at similar rates) was desirable. We applied membrane stretch, stepped to test voltage X, and recorded the current. If stretch is strictly a surrogate for voltage, we reasoned, it should be possible to reproduce, without stretch, the same P_O time course at a voltage some millivolts more depolarized (X + ΔV).

Fig. 3 A illustrates a representative experiment: A recording at 50 mV with stretch was directly followed by 5aa recordings at stepwise increased depolarizations without stretch. To compare P_O time courses, currents were scaled to compensate for the increased driving force at higher depolarizations. Rising phases at 50 mV with stretch and 85 mV without stretch were completely scaleable, indicating the same time course of P_O rise (Fig. 3 B), but the current decline at 50 mV with stretch was much faster than that at 85 mV without stretch. (As Fig. 8 A il-

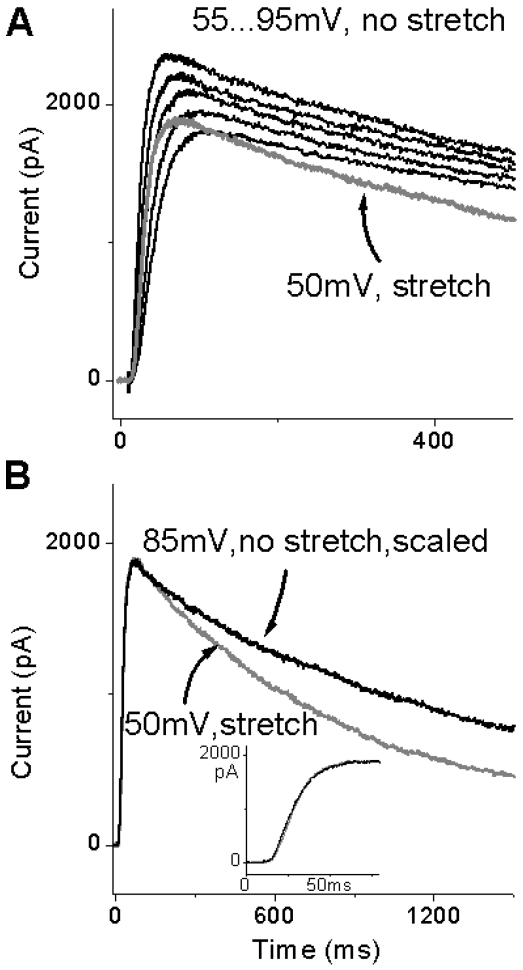

FIGURE 3. Trying to find a ΔV substitute for stretch. (A) 5aa currents evoked by stepping from −90 to 50 mV with −45 mm Hg suction (gray trace) and from −90 to 55–95 mV in 10-mV increments without suction (black traces). (B) The rising phases of the currents at 50 mV with stretch (gray) and 85 mV without stretch (black) are scaleable (inset, scaled currents on an expanded time scale). Downscaling was necessary to compensate for the increased driving force, but activation kinetics were otherwise identical: in its effect on channel activation, the 35-mV voltage increment was equivalent to the particular membrane stretch produced by −45 mmHg. Note, however, that compared with the accelerating effect of the stretch stimulus (at 50 mV), acceleration of inactivation by the depolarizing stimulus was less pronounced.

lustrates, under all conditions late current relaxed to the same vanishingly small level, validating this kinetic interpretation.) The inescapable conclusion is that as sources of gating energy, voltage and stretch are not completely interchangeable for all steps, so we now examine stretch effects on current rise and decline separately.

5aa Activation Appeared Simpler than WT Activation

Fig. 4 A shows a family of 5aa currents with maximum slope lines fitted to their rising phases (see MATERIALS AND METHODS), whereas Fig. 4 B plots the resulting delay and maximum slope as functions of voltage. The delay is well fitted by a single exponential, and the maximum slope by the inverse of the same function, multiplied by a linear function of voltage to account for driving force and channel conductance.

A simple 4-step activation model (each of four subunits undergoes an irreversible activation transition, and the channel is open when all are activated) produces that kind of behavior. Using this model to describe activation kinetics does not imply that subunits can undergo no other individual or concerted transitions, but simply that one transition per subunit is rate limiting for the entire activation gating process. The model translates into

$$C_0 \xrightarrow{4\alpha} C_1 \xrightarrow{3\alpha} C_2 \xrightarrow{2\alpha} C_3 \xrightarrow{\alpha} O$$

SCHEME I

What about deactivation reactions? For the reversible four-step model, steady-state $P_{0,\infty} = [1/(1+\beta/\alpha)]^4$, with voltage-dependent activation and deactivation rates α and β. Half maximal steady-state activation is reached for $\beta/\alpha = \sqrt[4]{2} - 1 \approx 0.19$. The midpoint voltage of the 5aa g(V) relation (Gonzalez et al., 2000) is ~0 mV. Thus, for voltages positive to 0 mV, activation is >5× faster than deactivation, which may be ignored in a first approximation. Note that Gd^{3+} (used in stretch experiments) right-shifts Shaker g(V) curves (Gu et al., 2001). In APPENDIX A(2) we discuss how deactivation affects delay and maximum slope versus voltage relations.

The open probability time course for the irreversible 4-step model,

$$P_O(t) = (1 - e^{-\alpha(V)t})^4, \tag{2}$$

has maximum slope and delay given by

$$S^P_{Max} = \left(\frac{3}{4}\right)^4 \alpha(V) \tag{3}$$

and

$$t_d = \frac{1}{\alpha(V)}\left(\ln 4 - \frac{3}{4}\right). \tag{4}$$

S^P_{Max} has superscript P (for probability) to distinguish it from the maximum slope S_{Max} of the current, which is Eq. 3 multiplied by the driving force. The voltage dependence of S^P_{Max} and t_d is determined by the exponential voltage dependence of the activation rate $\alpha(V)$,

$$\alpha(V) = \alpha_0 e^{z_\alpha FV/RT} \approx \alpha_0 e^{z_\alpha 0.039\, mV^{-1} V}. \tag{5}$$

We approximated F/RT by 0.039 mV^{-1} (Faraday constant, F = 96500C/mol; gas constant. R = 8.134 J/mol K; temperature, T = 298K).

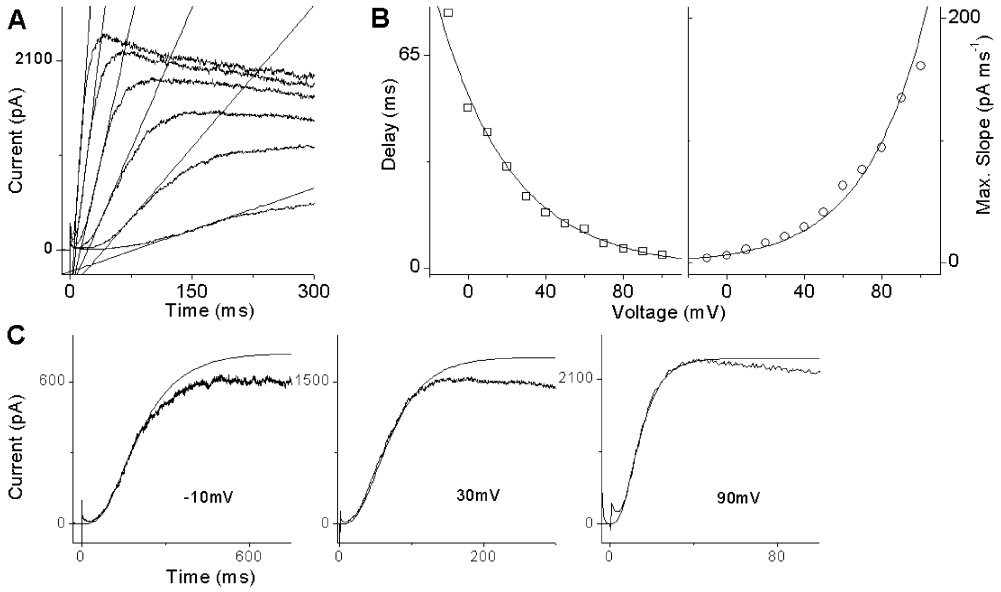

FIGURE 4. Voltage dependence of delay t_d and maximum slope S_{Max} for a family of 5aa currents evoked by stepping from a holding potential of −90 mV in 10-mV increments from −10 to 100 mV. (A) Sample currents (−10, 10, 30, 50, 70, 90 mV), with fitted maximum slope lines. (B) t_d (squares) and S_{Max} (circles) versus voltage. $t_d(V)$ can be fitted by a single exponential like Eq. 4, an expression from Scheme I. From the fit with Eq. 4, $z_\alpha = 0.68$ and $\alpha_0 = 12\ s^{-1}$ follow. The corresponding expression for S^P_{Max} in Scheme I is Eq. 3. To describe $S_{Max}(V)$, the voltage-dependent driving force has been included by multiplying Eq. 3 with (V + 90 mV) and a constant. This, with the gating charge from the $t_d(V)$ fit, yields a satisfying description of $S_{Max}(V)$. (C) Fitting current rising phases with Eq. 4. Sample currents at −10, 30, and 90 mV from the current family in A. P_O(t) from Eq. 2, with α_0 and z_α from the $t_d(V)$ fit in B, has been scaled to match the rising phases—the irreversible four-step model describes the current rise well. The remainder of the capacitive transient at 90 mV is unlikely to obstruct determination of channel current properties (see Fig. 1).

Conformational changes during S4 movement and channel opening are discontinuous motions, a succession of fast transitions over energetically (sterically and electrostatically) unfavorable states, plus relatively long sojourns in more stable states (Bezanilla, 2000). If the total gating charge moved during a subunit conformation change with forward rate α is z, then z_α (in Eq. 5) is the part of z moved during transformation into the transition state from the stable conformation further from the open state. Only z_α influences the forward rate, since the rest of the transition is energetically downhill and thus fast. $z_\beta = z - z_\alpha$ then determines the voltage dependence of the back transformation rate.

Shaker WT activation models (more activation steps per subunit, additional concerted pore opening steps) do not generally produce monoexponential $t_d(V)$ and $S^P_{Max}(V)$ relations (unpublished result). Later we discuss effects of some model additions on $t_d(V)$ and $S^P_{Max}(V)$. The diminished S3–S4 linker of 5aa might simplify its activation by making one transition per subunit rate-limiting for opening. Interpreted in the context of the four-step model, delay and maximum slope monitor this rate-limiting step; the Eq. 3 fit of $t_d(V)$ in Fig. 4 B yields estimates for α_0 and z_α, of 12 s^{-1} and 0.68, respectively. Obviously, four times this z_α is only a fraction of the total 12–13 electronic charges moved during Shaker gating (e.g., Schoppa et al., 1992). For WT, Zagotta et al. (1994a) also obtained relatively small gating charges for single activation and deactivation steps and so concluded that charge movement was spread among many activation transitions. With our method, we observe only transitions that shape activation kinetics. Transitions faster than the rate-limiting ones influence neither opening kinetics nor the voltage dependence of $t_d(V)$ and $S_{Max}(V)$, thus the gating charge they contribute goes unnoticed. Interestingly, too, the fit of the 5aa g(V) relation with a fourth order Boltzmann yields a gating charge of only four times 1.65 electronic charges, which would be $z_\alpha + z_\beta$ of the rate-limiting activation step (Gonzalez et al., 2000).

The kinetic simplicity of 5aa activation was probed further by testing how well the current rising phase was fitted by Eq. 2 (i.e., P_O(t) for Scheme I) using parameters obtained from the $t_d(V)$ fit. This is done in Fig. 4 C for sample currents from Fig. 4 A using α_0 and z_α from the $t_d(V)$ fit shown in Fig. 4 B. The four-step model fits the rising phases well at all voltages, indicating that Scheme I adequately describes 5aa activation kinetics. Because currents from some patches were less clear-cut, we later show how inactivation, deactivation, additional activation steps per subunit, and concerted steps would affect our ability to fit simulated $t_d(V)$, $S^P_{Max}(V)$ and P_O(t) using the irreversible four-step model.

However, in eight of eight patches without stretch, $t_d(V)$ was well-described with Eq. 4 and $z_\alpha = 0.64 \pm 0.02$ (mean ± SEM). In six of those eight, $S_{Max}(V)$ was well described by the same exponential function (multiplied by a constant and $(V + 90\ mV)$ for the driving force). In one case, $S_{Max}(V)$ could not be described by a single exponential, in another the fitted single exponential had

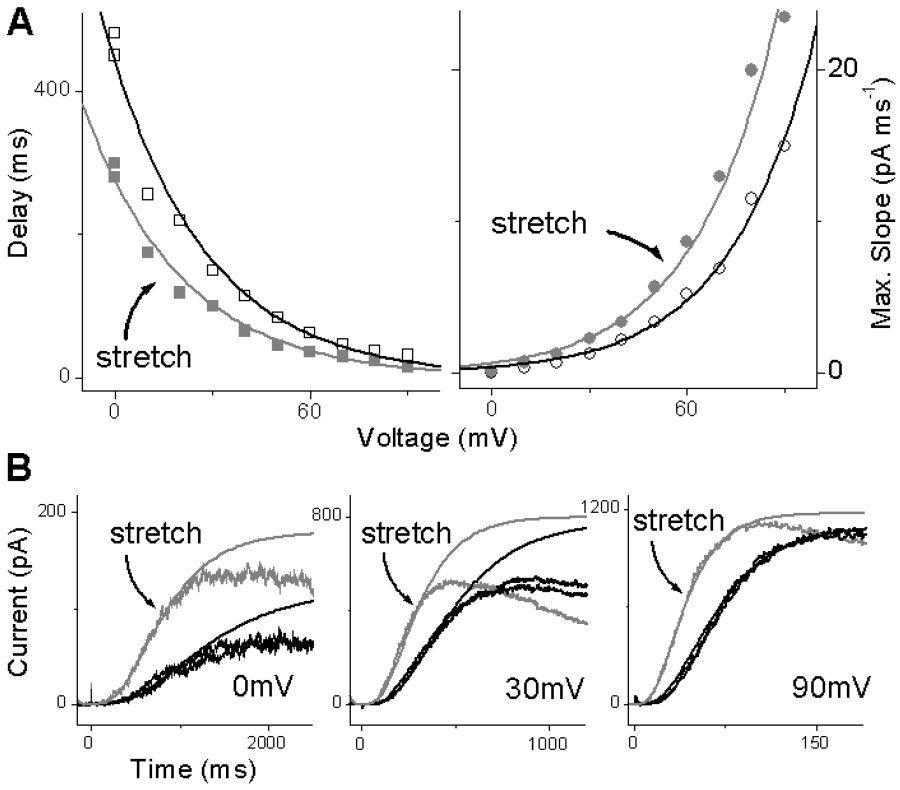

FIGURE 5. The four-step model describes 5aa current properties with and without stretch. (A) Delay and maximum slope from 0 to 90 mV, with (gray symbols) and without −45 mm Hg suction (open symbols); voltage was stepped to the indicated levels from −90 mV. $t_d(V)$ without stretch is fitted with Eq. 4, $\alpha_0 = 1.4\ s^{-1}$ and $z_\alpha = 0.85$. With stretch, the same z_α, and $\alpha_0 = 2.3\ s^{-1}$ provide a good description. $S_{Max}(V)$ with and without stretch is well described by Eq. 3, multiplied by a linear driving force, and with the z_α value from the delay fit. (B) Sample currents with (gray) and without stretch, before and after (black). P_O(t) from Eq. 2 with z_α and α_0 from the $t_d(V)$ fits in A has been scaled to match the current rise.

a different exponent. The estimates of α_0 from the $t_d(V)$ fit ($8.9\ s^{-1} \pm 1.4\ s^{-1}$) varied with a negative correlation ($r = -0.46$) between α_0 and z_α. Temperature variations might explain this since α_0 will increase with temperature while z_α will seem smaller: a temperature-related exponent decrease in the fits of Eqs. 3 and 4 to experimental $t_d(V)$ and $S_{Max}(V)$ will decrease the resulting z_α, which we calculate assuming 298°K (see Eq. 5). Oocyte batch–dependent membrane properties might also affect α_0. In any case, it is reassuring that z_α, representing gating charge, was less variable.

For four of eight current families, Eq. 2 with z_α and α_0 from the fit of their $t_d(V)$ described well at all voltages both the current rising phases and current amplitudes at large depolarizations. In two other families the rising phases were well fitted at all voltages, but Eq. 2 did not reproduce amplitude saturation at large depolarizations (see Fig. 9 B, insets, in APPENDIX). In another case, at mild depolarizations, the amplitude of an Eq. 2 fit that matched the initial current rise was smaller than the current amplitude (see Fig. 11 B, insets).

Stretch Effects on Activation Kinetics

Fig. 5 A shows $t_d(V)$ and $S_{Max}(V)$ for currents at 0–90 mV with and without stretch. At all voltages, stretch increased the maximum slope and decreased the delay. The exponential voltage dependence of t_d and S_{Max} was preserved and, moreover, could be described with the same exponent for both functions, with and without stretch. This strongly indicates that both stretch and voltage act on the rate-limiting activation step, with stretch increasing α_0, the subunit activation rate at 0 mV. This sensitivity of α_0 points to a stretch-induced decrease in the conformational energy barrier between the two stable voltage sensor states of the rate-limiting gating transition. There may be stretch effects on transitions in the voltage-dependent activation path too fast to shape current kinetics. We can, however, exclude the possibility of another, solely stretch-activated opening pathway. In that case, stretch would affect the voltage dependence of S_{Max} and t_d differently, change the voltage-dependent exponential or, very likely, render the voltage dependence nonexponential.

Fig. 5 B shows fits of P_O(t) (Eq. 2) to currents from Fig. 5 A, with α_0 and z_α from the $t_d(V)$ fits there. Those fits capture the early rising phase, but at the lower voltages the current deviates from the scaled P_O(t) earlier than in the example without stretch in Fig. 4, probably because α_0 without stretch was ~8 times slower in Fig. 5 B than in Fig. 4, so inactivation would have more strongly influenced the current rising.

In five such experiments, $t_d(V)$ and $S_{Max}(V)$ with and without stretch were well-described by exponentials with the same exponent z_α (multiplied by a linear driving force term for $S_{Max}(V)$). z_α was 0.71 ± 0.10 (mean ± SEM), similar to the value obtained for the eight patches not subjected to stretch (0.64 ± 0.02) (by *t* test, the two means have ~60% probability of being from

the same distribution). Again, α_0 was more variable: $\alpha_0 = 7.7\ s^{-1} \pm 4.4\ s^{-1}$ without stretch and $19.5\ s^{-1} \pm 13.5\ s^{-1}$ with. Although stretch was always applied via −45 mm Hg suction, tensions would differ among patches. The SEM of α_0 was made large by one experiment (α_0 = 25 s^{-1} without, 73 s^{-1} with stretch and z_α = 0.43—an example of the above-mentioned correlation between large α_0 and small z_α). In four of five patches, current rising phases with and without stretch were satisfyingly fitted with Eq. 2, using z_α and α_0 obtained from fits of $t_d(V)$. As in Fig. 5 B, the fits reproduced the initial current rise. They overestimated the later amplitudes at small depolarizations, but approximated the full activation time course at large ones. In the fifth experiment, the fit underestimated current amplitude at moderate depolarizations and exceeded it at large ones.

Considering Some Realistic Model Additions

We have illustrated successful attempts to explain 5aa activation over a voltage range with and without stretch with the four-step model in Scheme I. Usually $t_d(V)$ and $S_{Max}(V)$ were well fitted with the exponentials in Eqs. 3 and 4, and current rise could be described by scaled versions of P_O(t) from Eq. 2, using the parameters from the delay fit. Given the (relatively fast) "slow" inactivation of 5aa, one would not expect Eq. 2 to reproduce current rise and final amplitude at mild depolarizations, and it is satisfying that at large ones (saturated P_O) the fit and current amplitudes were often identical. In APPENDIX A, however, we consider two issues. (1) Might activation kinetics really be substantially different and only accidentally described by the four-step model? (2) Even though Eqs. 3 and 4 usually described $t_d(V)$ and $S_{Max}(V)$ with/without stretch satisfyingly, for some recordings Eq. 2, with the parameters from the delay fit, failed to reproduce at large depolarizations the combination of current rise and amplitude.

As an attempt to explain such failures while keeping an eye to issue 1, we consider the impact of some realistic additions to Scheme I: inactivation, deactivation reactions, cooperative last activation steps, and finally, more activation steps per subunit. Some of these extended models do not yield analytical expressions for $t_d(V)$ and $S_{Max}(V)$. Others do, but with more unknown parameters than Eqs. 3 and 4, making their fits to the experimental delay and maximum slope relations less meaningful. Instead of trying to fit our data with the latter models, our strategy is to take their output—simulated $t_d(V)$ and $S_{Max}(V)$ relations—and try to fit them with the expressions from the irreversible four-step model, looking for signature inadequacies in the fits that might resemble inadequacies observed when fitting our experimental data.

Thus, we eventually exclude some extended models and make a case for others. We never observed behavior characteristic for an activation pathway with more than one kinetically significant step per subunit. We also exclude five-step models with voltage-independent final concerted steps. To explain most of our data, and even most deviations encountered from the behavior of the basic four-step model, a simple irreversible four-step model with inactivation from the open state (see Scheme II) is completely sufficient. We cannot, however, exclude an additional voltage-dependent final concerted step (with gating charge similar to z_α), though its effect on current activation properties is practically indistinguishable from that of inactivation (which is, in any case, required to explain the fast current decline). We also cannot fully exclude a contribution from deactivation reactions; they may explain rarely encountered deviations of our data from expectations of Scheme I (see Figs. 10 and 11 B, insets).

Slow Inactivation in 5aa

5aa currents are transient, with characteristic decline times comparable to those of WT. Having acknowledged that inactivation can affect current rise, we ask how activation might affect the falling phase, using a simple model of 5aa inactivation (Scheme II), in which "inactive" can only be reached via "open". Inactivation from states with closed activation gates may occur for Shaker WT (Klemic et al., 2001), but 5aa currents did not show the characteristic minimum in decline rate indicative of this "U-type inactivation".

In the most extreme case (rate-limitation of genuinely fast channel inactivation by slow activation) the inactivation rate i has no influence on current kinetics. If activation and inactivation rates are similar, both shape current rise and decline in a multiexponential fashion (Hille, 2001). Finally, if inactivation is slower than activation, the inactivation rate will be the main determinant of falling phase kinetics and what little influence the activation rate still has dies away with increasing depolarization. Which of the three regimes describes the falling phase of 5aa currents? A brief model analysis shows how to answer this question. We extend Scheme I by one inactivation step:

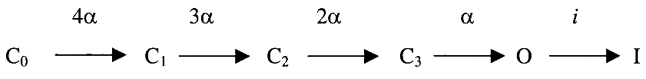

SCHEME II

The resulting time course of $O(t)$ (and the related P_O(t)) is a sum of exponentials. See APPENDIX B for a discussion of activation's influence on the current falling phase in the three regimes $i >> \alpha$, $i \approx \alpha$ and $i << \alpha$. In a nutshell, for $i << \alpha$, $O(t)$ kinetics are solely determined by multiples of the rate α. Normalizing the currents and rescaling the time then completely maps $O(t)$ time courses for different voltages (see Eq. A6), a

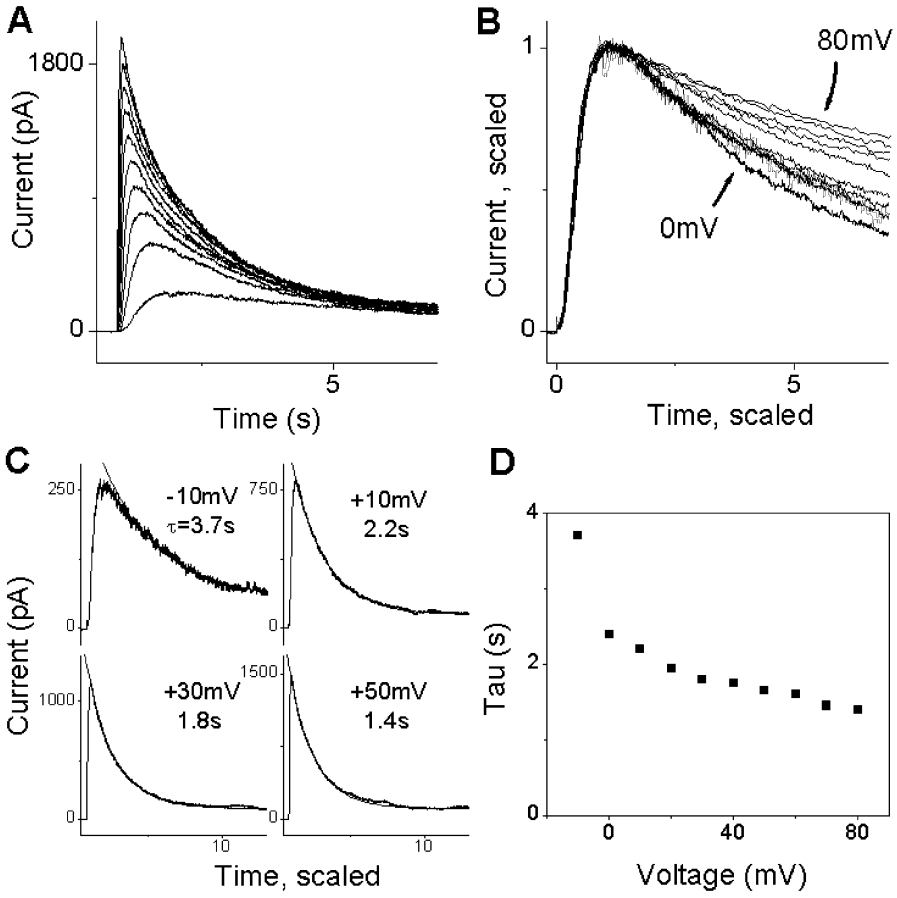

FIGURE 6. 5aa slow inactivation. (A) In a typical experiment (15 μM Gd^{3+} in the pipette) currents were evoked by stepping from a holding potential of −90 mV in 10-mV increments from −10 to 80 mV, and recorded on a long time scale. (B) Currents from A. Amplitudes are normalized and the time scaled for each voltage so the rising phases overlap. Activation cannot be rate limiting for inactivation, because the scaled decline slows progressively with increasing voltage, with the sole exception of the response at −10 mV (the noisy, lighter colored trace). (C) The current falling phases can be fitted by Eq. 1. The time constant τ of the monophasic exponential decay to a constant plateau is given on each panel. (D) $\tau(V)$ declines with increasing voltage.

property that distinguishes this inactivation regime from the others.

Fig. 6 A shows a typical current family at −10 to 80 mV. In Fig. 6 B, currents are normalized, with times rescaled to match the rising phases. If inactivation were rate limited by activation, the currents would overlap completely. Instead, there was a progressive slowing of the scaled falling phase with increasing voltage. Evidently, a less voltage-dependent process than activation largely governed the current decline. The current falling phases are well described by the exponential decline in Eq. 1, as illustrated in Fig. 6 C for unscaled currents at several voltages. The late current plateau likely originated in rare returns from the inactive to the open state (neglected in Scheme II). Fig. 6 D shows the decline time constant (τ in Eq. 1) as a function of voltage. The current decline rate increased only 1.5-fold between 0 and 80 mV, while the activation rate increased eightfold.

Current properties like in Fig. 6—exponential falling phases with weakly voltage-dependent τ, decline not rate limited by activation—were typical, with eight of nine families (no stretch) showing all these features. The pattern illustrated in Fig. 6, B–D, strongly argues against rate limitation of the current decline by activation ($i >> \alpha$), as does the finding (Gonzalez et al., 2000) that 5aa P_O saturation starts around 50 mV ($i >> \alpha$ and P_O saturation are mutually exclusive, see APPENDIX B). Experiments with stretch (see below) had Gd^{3+} (which right-shifts Shaker g(V) relations (Gu et al., 2001)), but we still expect P_O saturation near the range of voltages studied. For large depolarizations, inactivation must be in the $i \cong \alpha$ or $i << \alpha$ mode. If $i << \alpha$, $\tau(V)$ must reflect genuine voltage dependence in i. For $i \geq \alpha$, voltage dependence of i is not required to explain that of τ. If τ keeps decreasing for voltages beyond P_O saturation, i must be voltage dependent. Unfortunately, it is uncertain if P_O saturated in experiments like that in Fig. 6, i.e., for voltages less depolarized than 80 mV. Arguing against an influence of activation on the falling phase above ~0 mV, and in favor of (weakly) voltage-sensitive inactivation, is the monoexponential decline of the current falling phases (see Fig. 8 C).

Stretch Effects on Slow Inactivation

As Fig. 3 illustrated, stretch dramatically accelerated the current falling phase. As summarized there, a certain voltage increment that reproduced the stretch-induced

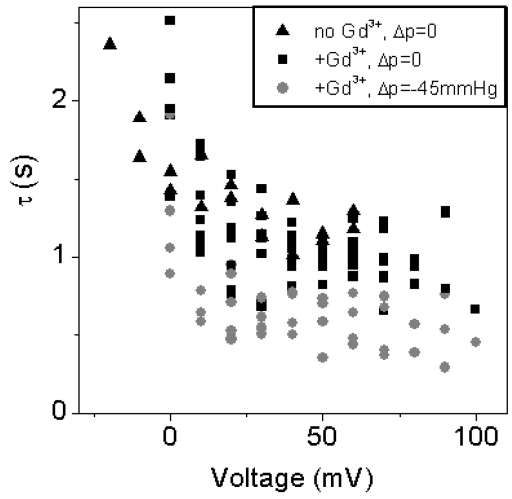

FIGURE 7. Voltage dependence of the time constant τ from fits of Eq. 1 to current falling phases, with and without stretch, pooled from a number of experiments. Most data were obtained with 10–20 μM Gd^{3+} in the pipette, but some data without Gd^{3+} are also shown, as indicated. Stretch reduced τ at all voltages. Gd^{3+} had no discernible effect, but since it right shifts the g(V) relation (Gu et al. 2001), time constants could be obtained at −10 and −20 mV without Gd^{3+} but not with it.

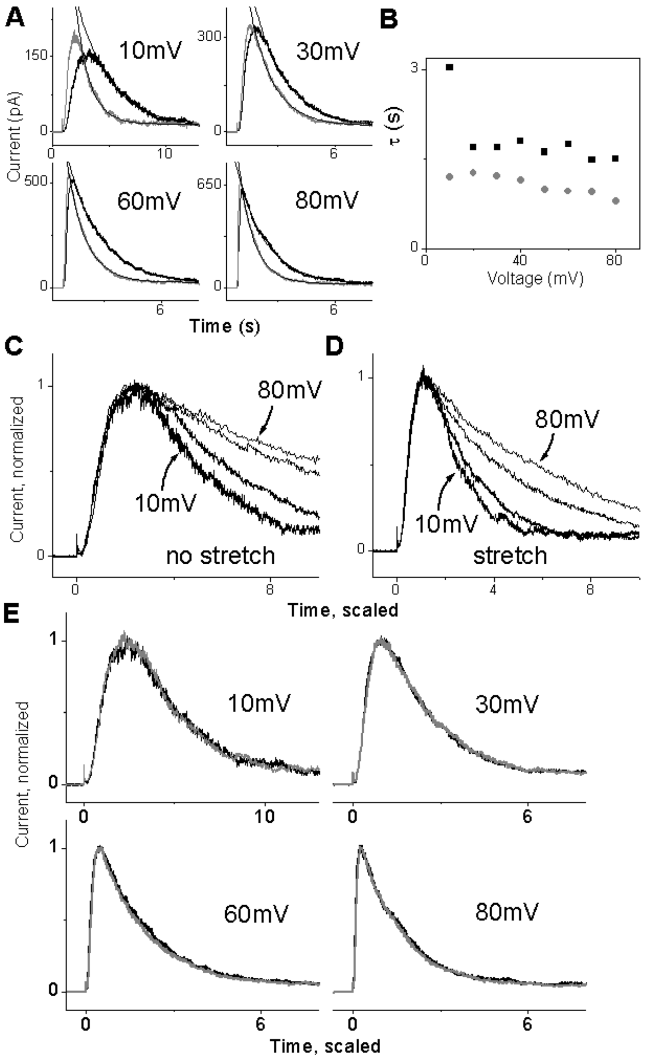

FIGURE 8. 5aa current decline and stretch. (A) Sample currents with and without −45 mm Hg suction. The falling phases have been fitted with Eq. 1. Stretch decreases τ. (B) τ *(V)* with (gray circles) and without stretch (black squares). (C and D) The sample currents with and without stretch from A have been normalized, their times scaled to match all rising phases. The scaled falling phase decelerates with increasing voltage. Above 10 mV, where the falling phase is not rate limited by activation, the inactivation rate dominates falling phase dynamics. (E) Normalized currents with and without stretch. For each voltage, the time scale of the current with stretch has been expanded to match the rising phase of the current without stretch. Note that the entire scaled time courses are virtually identical. C and D showed that activation is not rate limiting for the current decline at these voltages and thus stretch, in contrast to voltage, seems to affect activation and inactivation in exactly the same way.

acceleration of current activation did not reproduce that of the falling phase: slow inactivation must be directly stretch sensitive and, compared with activation, proportionately more stretch than voltage sensitive. Fig. 7 plots falling phase $\tau(V)$ and despite scatter (τ was extremely variable, sometimes even within a patch), a clear separation of values with and without stretch emerges.

Fig. 8 depicts an experiment like that in Fig. 6, except currents were recorded both with and without stretch. Current falling phases with and without stretch are fitted with Eq. 1 in Fig. 8 A. Stretch increased τ (Fig. 8 B), producing a similar speeding of the current falling phase at all voltages. This further indicates that stretch effects on current decline cannot be entirely mediated via accelerated activation, which must wane as P_O saturates with depolarization. Fig. 8, C and D, show normalized currents from A without (Fig. 8 C) and with (Fig. 8 D) stretch, with times scaled so the rising phases of all currents match the rise at 10 mV. With or without stretch, current decline above 10 mV was not rate limited by activation. The progressive slowing of the decline with depolarization indicates that a less voltage-dependent rate—the slow inactivation rate i—progressively dominated the current decline.

Finally, Fig. 8 E shows a striking result. At each test voltage, a simple rescaling of the time in case of the stretch current convincingly maps the normalized currents with and without stretch on each other. Without the results in Fig. 8, C and D, one might regard this as a sign that the entire P_O time course was determined by the activation rate α and its multiples ($i >> \alpha$, see APPENDIX B, Eq. A6), and that the stretch sensitivity of the current time course was purely mediated by that of α: Rescaling the time takes care of all stretch-induced kinetic changes, because they are caused by the same change in α. But Fig. 8, C and D, showed that the inactivation rate did

have an influence on current decline above 10 mV. Current kinetics are described by Eq. A7—there is a new exponential component with rate *i*. If stretch increased α, but not, or differently, *i*, then a rescaling of the time could not match the exponential components in the stretch and no-stretch curves, and the currents would not overlay completely. Since they do, we must conclude that stretch affected the inactivation rate in exactly the same way as α—e.g., if α is doubled by stretch, *i* doubles too. We tested 10 patches for the occurrence of this surprising pattern. The match was nearly perfect across all voltages in four patches, showed only minor deviations of the scaled time courses in four others, and there was no match in two. Eq. A7 does not yield a change in P_O for proportional changes in α and *i* but we did observe reversible amplitude increases by stretch, perhaps because stretch increases channel conductivity, but more likely, because it also alters the equilibrium of additional nonrate limiting activation steps.

We could dismiss the proportional stretch acceleration of activation and inactivation as coincidental, and simply retain the conclusion that inactivation, too, must be stretch sensitive. Alternatively, we can speculate about shared properties of activation and inactivation. A simple explanation for their identical response to stretch would be that the rate-limiting steps in activation and slow inactivation both involve expansion of the channel protein in the plane of the bilayer, which is likely to be facilitated by lipid decompression caused by membrane stretch.

DISCUSSION

Overview

We studied the stretch and voltage dependence of activation and slow inactivation in a Shaker deletion mutant, 5aa. Though 5aa and Shaker WT differ in that 5aa has 26 fewer residues in the S3–S4 linker than WT, two points are noteworthy: (a) most eukaryotic voltage-gated K channels have 10–20 fewer residues in this region than Shaker WT, and (b) ~10 linker residues is the norm for six transmembrane voltage-gated channels (e.g., prokaryotic Na; Ren et al., 2001b) and K (Jiang et al., 2003a) channels, and eukaryotic cation (Ren et al., 2001a) and hyperpolarization-activated cyclic nucleotide–gated (Gauss et al., 1998) channels). 5aa was chosen for kinetic scrutiny because both the rise and fall of its currents are reversibly sensitive to membrane stretch and because the two processes occur on comparable timescales and so could be monitored during the same stretch stimulus in any given patch. Moreover, the slow activation of 5aa relative to passive charging times facilitated resolution of early currents. The goal was to determine, from a kinetics standpoint, whether the voltage-dependent transitions of this class of channel are inherently susceptible to the level of membrane tension. Macroscopic cell-attached patch currents were examined without and with stretch, with membrane tension increased reversibly by patch suction. The fact that membrane tension in a given patch was not quantified was not a major shortcoming because analyses were designed around tests at several voltages for each patch before, during and after a fixed level of pipette suction. As was hoped, simultaneous application of within-patch comparisons to both of two putatively stretch-sensitive kinetic processes, activation and slow inactivation, proved to be particularly worthwhile. Our intent was not to quantify the mechanical contribution of stretch to gating (this has been done in a rudimentary fashion, Tabarean and Morris, 2002) but to identify tension sensitive transitions. Gonzalez et al. (2000) showed that 5aa is kinetically simpler than the parent molecule, making it attractive for extracting microscopic kinetic information from macroscopic currents. Because of the relative simplicity of 5aa gating compared with WT we could seek a parsimonious description of the rate-limiting steps and the kinetic "site" of stretch sensitivity in the two processes of interest, activation and inactivation. In this context, the question of whether gating currents are stretch sensitive is extremely interesting, but achieving channel densities that would permit gating currents to be recorded from patches with and without stretch would be difficult.

For activation, the voltage dependence of current delay (t_d) and maximum slope (S_{Max}) was the same with and without stretch. We interpret the single exponential form of this voltage dependence as reflecting a simple four-step activation pathway with one rate-limiting activation step per subunit. The conservation of general form and voltage dependence of S_{Max} and t_d with and without stretch signifies that stretch and voltage act on the same rate-limiting activation steps. Stretch might additionally influence activation steps (e.g., pore opening) that are not rate limiting in 5aa, but our kinetic approach does not monitor them. We discussed the input of several model extensions, the most important of which is slow inactivation, whose influence on activation characteristics explains most of the encountered deviations from the behavior of the simple four-step model.

Quantifying the voltage dependence of 5aa slow inactivation is challenging because the current falling phase may be contaminated by events in the activation pathway. Moreover, inactivation can be variable even within a patch. However, voltage dependence in the decline time constant persisted even at very depolarized voltages, where decline is likely not influenced by activation.

For Shaker WT excised patches with high Na and low K at the intracellular face, Starkus et al. (2000) suggested that at positive voltages the voltage dependence

of the decline time constant arises from increased Na permeability. K in the pore inhibits inactivation (Lopez-Barneo et al., 1993), so displacing it with Na might speed inactivation. In our experiments, this might contribute to whatever part of the voltage dependence of inactivation was not activation mediated, but it is unclear if the Starkus et al. (2000) effect applies for the physiological ionic conditions used here. A U-shaped voltage dependence of inactivation, with maximal inactivation speed at 0 mV, has been reported by Klemic et al. (2001) for Shaker WT, who propose a model involving inactivation from closed states, but we detected no sign of U-type inactivation in 5aa.

Stretch Susceptibility of 5aa in Light of Sensor Motion Models

In the paddle model (Jiang et al., 2003a), the voltage sensor moves through lipid rather than inside the generally accepted (e.g., Horn, 2002) gating canal. Interestingly, deletion in 5aa of 26 residues between S3 and S4 render its primary sequence far closer to KvAP through this part of the protein than is WT Shaker. The paddle would be dragged through lipid from a closed position almost perpendicular to the pore to the open (then inactivated) position almost parallel to the pore. While this implies substantial lipid displacement during gating it is unclear if a net expansion in the plane of the bilayer is expected. "Gating canal" models of sensor motion are also silent on whether activation would involve net expansion of the channel protein (e.g., Bezanilla, 2002; Gandhi and Isacoff, 2002; Horn, 2002), but as we have emphasized (Tabarean and Morris, 2002), expansion by only a few percent would suffice to explain Shaker stretch sensitivity.

Voltage-gated K-channel gating kinetics slow with hyperbaric pressure (Conti et al., 1982; Meyer and Heinemann, 1997). This may be the reciprocal of the effect of membrane stretch (Tabarean and Morris, 2002). Hyperbaric pressure effects on channel gating are generally interpreted in terms of protein compression and hence of reduced activation volumes (e.g., Macdonald, 2002). Somewhat overlooked is the fact that, because of increased chain ordering, bilayer compression is anisotropic and so high pressures yield a thicker bilayer (Scarlata, 1991). Insofar as stretch thins the bilayer, the reciprocity of elevated pressure/elevated bilayer tension may relate to increased/decreased membrane thickness at the channel–bilayer interface. For either an expanding channel or a voltage-sensor paddle moving through the membrane, displacing lipids should be slower in a thicker more orderly bilayer. Mechanosensitivity and the slowing of both activation and inactivation in human T lymphocyte Kv1.3 channels by high membrane cholesterol (Hajdu et al., 2003]) could have common explanations.

Our findings (like those with cholesterol; Hajdu et al., 2003) are consistent with the possibility that inactivation involves voltage sensor movement, as suggested from the voltage clamp fluorometry of Loots and Isacoff (2000). Merely from the isolated rates, we need not demand that stretch act on activation and inactivation via the same mechanism. Strikingly, however, the kinetics with and without stretch matched after a simple rescaling of the time axis: stretch seems to affect activation and inactivation in a concerted fashion. Since inactivation was not rate limited by activation, this concerted action seems most explicable if both transitions involve, e.g., an expansion of the channel protein, or movement of the same structural groups. There is, of course, an apparent contradiction because the weak voltage dependence of inactivation (compared with activation) does not fit with the substantial voltage sensor movement perpendicular to the electric field needed to explain activation. A hypothesis that could unify the apparent contradictions and predict the stretch-and-voltage sensitivity pattern of 5aa would be this: inactivation and the rate limiting step of activation involve similar degrees of lateral voltage sensor motion, hence their common stretch sensitivity, but the activation motion entails substantially more perpendicular charge movement (e.g., from helix rotation) than does the inactivation motion.

APPENDIX A

Different Model Extensions and How They Influence $t_d(V)$, $S_{max}(V)$, and $P_O(t)$ and the Quality of Fits Using Scheme I

In each case, we simulate data for an extended model and try to fit these "data" with the irreversible four-step model expressions.

1. Inactivation

In the body of the paper we interpreted amplitude discrepancies between recorded current rises at moderately depolarized voltages and their fits with Eq. 2 as inactivation effects. Generally, for similar rates of 5aa "slow" inactivation and activation in the Scheme II model, inactivation slows the current rise as soon as channels begin to open. The first latency of channel opening would be unaffected by this, but our delay is defined by the intersection of the maximum slope line with the time axis. Inactivation reduces the maximum

TABLE I

Activation Parameters

	No Stretch (eight experiments)	Stretch (five experiments)
z_α	0.64 ± 0.02	0.71 ± 0.2
α_0	8.9 ± 1.4 s^{-1}	19.5 ± 13.5 s^{-1}

Results for z_α and α_0 (mean ± SEM) from the fits of Eqs. 3 and 4 to $t_d(V)$ and $S_{max}(V)$. Data from a number of experiments, each comprising current recordings at different voltages from one patch, with and without stretch.

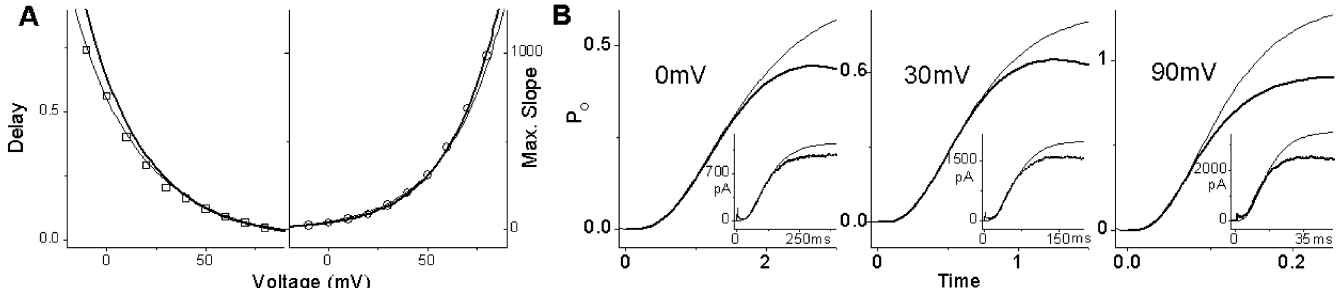

FIGURE 9. Influence of inactivation on our analysis. (A and B) Simulated kinetic data for a model with four irreversible activation steps plus inactivation (Scheme II). $\alpha_0 = 1$, $z_\alpha = 0.85$, inactivation rate $i = 0.5$ (arbitrary units). (A) Simulated $t_d(V)$ and $S_{Max}(V)$ relations, from fits of maximum slope lines to simulated P_O(t) (symbols). For comparability with the experimental results, simulated S^P_{Max} in Figs. 9–13 have been multiplied by (V + 90 mV) to mimic a driving force. Thick lines, predicted delay and maximum slope without inactivation ($i = 0$). This line (delay), fit of $t_d(V)$ with Eq. 3, $\alpha_0 = 1.15$ and $z_\alpha = 0.76$. Thin line (slope), fit of the maximum slope with Eq. 2 and z_α from the delay fit. (B) Simulated P_O(t) (thick lines) and fits with Eq. 2, α_0 and z_α from the delay fit (thin lines). The fits look reasonable at low voltages. At 90 mV, $\alpha(V)$ predicted from the fit of $t_d(V)$ is too slow. To fit the simulated rise, Eq. 2 must be upscaled beyond the peak P_O amplitude. (B, insets) Sample currents from an experiment. Currents and their fits with Eq. 2 and the apparent parameters from the delay fit ($\alpha_0 = 15\ s^{-1}$, $z_\alpha = 0.58$, not depicted) behave like the simulated data in that they show the same failure to reproduce P_O saturation at large voltages.

slope and thus shifts t_d to earlier times. Coupling between maximum slope and delay seems intrinsic to every macroscopic delay measure. Note that the effect of inactivation is not like downscaling the entire current, which leaves t_d unchanged.

For voltage-independent or weakly voltage-dependent inactivation, the inactivation effect on t_d and S_{Max} is most prominent at small depolarizations, where delays are large and maximum slopes small. Thus, effects may be overlooked in $S_{Max}(V)$, but $t_d(V)$ will be markedly shallower than without inactivation. Trying to fit this $t_d(V)$ with a formula that ignores inactivation will produce incorrect estimates of activation parameters.

Fig. 9, A and B, shows simulated activation data for Scheme II. In Fig. 9 A, simulated $t_d(V)$ and $S_{Max}(V)$ (with inactivation) can be fitted with Eqs. 3 and 4, but from the fit of $t_d(V)$ the true α_0 is overestimated, z_α underestimated. Eqs. 3 and 4 with the true parameters ($t_d(V)$ and $S_{Max}(V)$ without inactivation) are drawn for comparison. The simulated $S_{Max}(V)$ is adequately described by both genuine and apparent z_α values. Fig. 9 B shows attempts to describe simulated P_O(t) rise with Eq. 2 and the apparent parameters from the $t_d(V)$ fit. While the latter underestimate the voltage-dependent rise in the isolated activation rate $\alpha(V)$ for all voltages, the influence of inactivation on the P_O rise wanes for fast activation at large depolarizations. To reproduce the P_O(t) rise at these voltages with the slower apparent $\alpha(V)$, Eq. 2 must be upscaled, making P_O impossibly high at 90 mV—the fits don't reproduce the expected amplitude saturation. Two of eight experiments without stretch (example as insets in Fig. 9 B, $t_d(V)$ not depicted) yielded such behavior.

To summarize, P_O saturation at large depolarizations implies identical amplitudes of recorded currents and their fits by the irreversible four-step model. Failure to reproduce this saturation might indicate that Scheme I needs to be extended by an inactivation step. We observed such behavior (inset in Fig. 9 B), although not regularly, which could be explained by (voltage independent) variations in the ratio of activation and inactivation rates. Those were sometimes evident even in the course of experiments on a given patch (unpublished data).

2. Deactivation Reactions

Scheme I neglects deactivation, but all activation steps are reversible, with the deactivation steps' voltage dependence determined by z_β, the gating charge movement between the transition state and (for whatever two stable states are in question) the one closer to the open channel conformation.

$$\beta(V) = \beta_0 e^{-z_\beta 0.039\, mV^{-1} V}. \tag{A1}$$

(As in Eq. 5, we substituted 0.039 mV^{-1} for F/RT.) The reversible four-step model has a simple analytical solution for P_O(t), and also for $t_d(V)$ and $S^P_{Max}(V)$. With deactivation, $t_d(V)$ is generally nonmonotonic

$$t_d = \frac{1}{\alpha(V) + \beta(V)}\left(\ln 4 - \frac{3}{4}\right), \tag{A2}$$

with a maximum at

$$\bar{V} = \frac{1}{0.039\, mV^{-1}(z_\alpha + z_\beta)} \ln \frac{\beta_0 z_\beta}{\alpha_0 z_\alpha}. \tag{A3}$$

The voltage $\bar{V}$ of the t_d maximum depends on the ratio of the products of basic rate and gating charge, with $\bar{V}$ negative if $\beta_0 z_\beta < \alpha_0 z_\alpha$. Far from $\bar{V}$, $t_d(V)$ can be approximated by single exponentials, specifically by Eq. 4 for

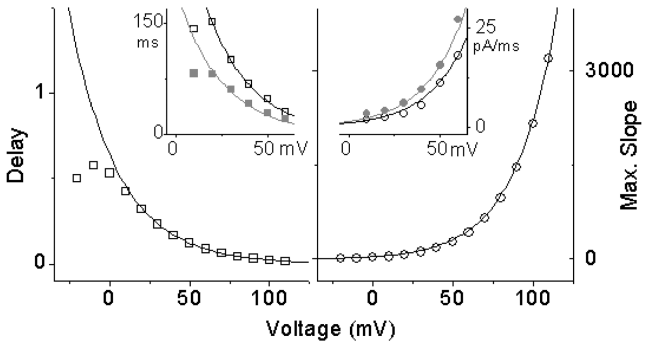

FIGURE 10. Effect of back reactions with $z_\beta < z_\alpha$ on $t_d(V)$ and $S_{Max}(V)$. Simulated data. $\alpha_0 = 1$, $\beta_0 = 0.2$, $z_\alpha = 0.85$, $z_\beta = 1.7$ (arbitrary units). From Eqs. A3 and A4, $\bar{V} \approx -9$ mV and $V_{1/2} \approx 0$ mV. Symbols, simulated $t_d(V)$ and $S_{Max}(V)$. Solid lines, predicted delay or maximum slope without deactivation (Eqs. 3 and 4). Simulated $S_{Max}(V)$ is indistinguishable from its counterpart for the irreversible model; simulated $t_d(V)$ is well described at large voltages, but bends characteristically below 0 mV. P_O(t) rise, and amplitudes (except at the lowest voltages) are well fitted by Eq. 2 (not depicted). (Inset) One of two observations of a bend in $t_d(V)$. Experimental $t_d(V)$ and $S_{Max}(V)$ relations with (gray symbols) and without stretch (open symbols). Delay fits (from which the bend region has been excluded) by Eq. 4, apparent $\alpha_0 = 1.9\ s^{-1}$ and $\alpha_0 = 3.3\ s^{-1}$ without and with stretch, respectively, $z_\alpha = 1$ for both. Maximum slope fitted with Eq. 3 (multiplied by linear driving force) and the same z_α. As in the simulated example, current rise and amplitudes were well fitted by Eq. 2 with the parameters from the delay fit, except at the lowest voltages, where amplitudes were smaller (not depicted).

$V >> \bar{V}$. How well this approximation works for voltages near $\bar{V}$ depends on the relative steepness of $\alpha(V)$ and $\beta(V)$. If $z_\beta > z_\alpha$, deactivation does not affect $t_d(V)$ at most $V > \bar{V}$, and there is a sudden bend in $t_d(V)$ near $\bar{V}$. If $z_\beta \leq z_\alpha$, deactivation retains influence on $t_d(V)$ also at $V > \bar{V}$. Eq. 4 would not fit $t_d(V)$, or the fit would yield wrongly estimated (apparent) values for α_0 and z_α.

Can we justify ignoring deactivation reactions in the kinetic analysis of 5aa currents? We looked for some indication of a maximum in $t_d(V)$. Because of signal-to-noise considerations, our lowest recording voltage was usually 0 or −10 mV. In 12 recordings of $t_d(V)$ down to 10 to −10 mV, there were only two instances of a $t_d(V)$ bend (Fig. 10, insets). Evidently the deactivation-related $t_d(V)$ maximum in 5aa occurs at very small depolarizations, where it is inaccessible because of vanishing current amplitudes. For $z_\beta > z_\alpha$, deactivation can be ignored for all but the smallest depolarizations.

Are our data compatible with $z_\beta > z_\alpha$? We define $V_{1/2}$, the midpoint voltage of the steady-state P_O for the reversible four-step model.

$$V_{1/2} = \frac{1}{0.039\,mV^{-1}(z_\alpha + z_\beta)} \ln \frac{\beta_0 \sqrt[4]{1/2}}{\alpha_0(1 - \sqrt[4]{1/2})} \approx \frac{1}{0.039\,mV^{-1}(z_\alpha + z_\beta)} \ln \frac{5.289\beta_0}{\alpha_0}. \quad \text{(A4)}$$

Ranges for $\bar{V}$ and $V_{1/2}$, two characteristic properties of the four-step model with deactivation, can be inferred from current recordings and the $t_d(V)$ derived from them respectively. Our experimental data provide clear guidelines: $V_{1/2} \geq 0$ mV (see also Gonzalez et al., 2000, $V_{1/2} \approx 0$ mV), and $\bar{V} < 0$ mV. These guidelines translate via Eqs. A3 and A4 into conditions for the 5aa activation and deactivation parameters. Is $z_\beta > z_\alpha$ compatible with the constraints $\bar{V} < 0$ mV and $V_{1/2} \geq 0$ mV? If $z_\beta > z_\alpha$, $\beta_0 < \alpha_0$ must be valid to keep $\bar{V}$ negative. With this condition fulfilled, there is a range of β_0 values producing positive $V_{1/2}$ for a given α_0 ($\alpha_0 > \beta_0 > \alpha_0/5.289$, see Eq. A4). With z_α around 0.7 (Table I) and z_β at least twice z_α, $\bar{V}$ calculated for a permitted α_0/β_0 combination cannot be below −12 mV: If $z_\beta > z_\alpha$, the $t_d(V)$ maximum should fall in the voltage range of the experimental $t_d(V)$ and be visible at least as a bend at the lowest recording voltages. Fig. 10 shows simulated $t_d(V)$ and $S_{Max}(V)$ for an example with $z_\alpha = 0.8$, $z_\beta = 1.7$, $\bar{V} \approx -9$ mV and $V_{1/2} \approx 0$ mV. $\beta(V)$ is negligible for most positive voltages, and $t_d(V)$ and $S_{Max}(V)$ are indistinguishable from the irreversible four-step model (thick line). Note the characteristic bend in $t_d(V)$. The inset in Fig. 10 shows one of the two above mentioned experimental instances of such behavior. Thus, we do not fully exclude deactivation with $z_\beta > z_\alpha$ in 5aa, but consider it unlikely based on the lack of examples for the expected bend in $t_d(V)$. However, if there is deactivation with $z_\beta > z_\alpha$, the estimates of α_0 and z_α from $t_d(V)$ fits with Eq. 4 are very close to the genuine values of these parameters. For the example in Fig. 10, Eq. 2 and the parameters from the delay fit provide good fits to simulated P_O(t) rising phases at all but the smallest depolarizations (unpublished data).

If $z_\beta \leq z_\alpha$ instead, the $\beta(V)$ approach to zero at positive voltages is shallow. Fig. 11 A shows $t_d(V)$ and $S_{Max}(V)$ for a simulated example of such conditions ($\bar{V} \approx -40$ mV and $V_{1/2} \approx 42$ mV). Deactivation noticeably affects delay and maximum slope: t_d is shorter and S_{Max} is smaller than without deactivation at all but the most depolarized voltages. A slight $t_d(V)$ bend starts around 0 mV. Simulated $t_d(V)$ may be fitted by Eq. 4 with apparent parameters, but the apparent z_α from the $t_d(V)$ fit does not describe the simulated $S_{Max}(V)$ very well. In Fig. 11 B, fits of the corresponding simulated P_O(t) with Eq. 2 and the apparent parameters from the $t_d(V)$ fit were attempted. The P_O(t) amplitude at 0 mV is very small due to the strong deactivation influence—though Eq. 2 has been strongly downscaled to match the P_O rise, the final fit amplitude still exceeds the small simulated amplitude. Interestingly, at 30 mV the simulated amplitude is undershot by the amplitude of the downscaled version of Eq. 2 that matches the simulated rise. At large voltages, the deactivation effect on P_O(t) wears off—the apparent rate extrapolated from the $t_d(V)$ fit is

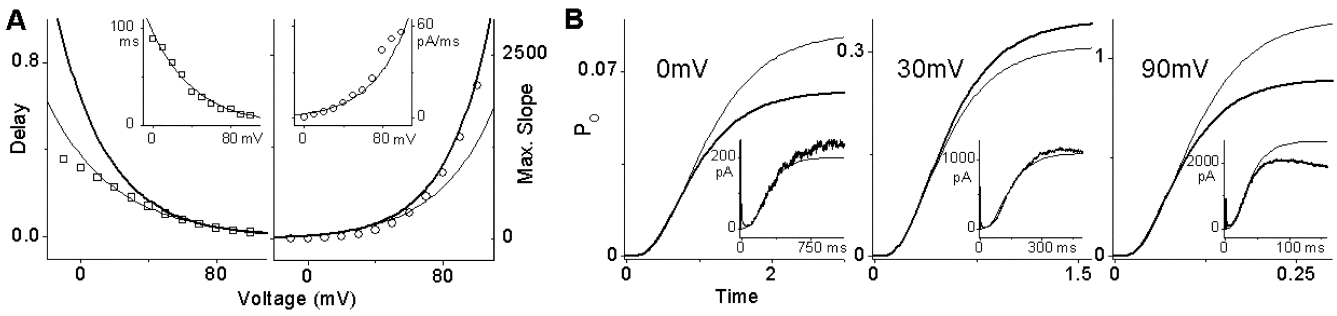

FIGURE 11. Effect of back reactions with $z_\beta < z_\alpha$. $\alpha_0 = 1$, $\beta_0 = 1$, $z_\alpha = 0.85$, $z_\beta = 0.17$ (arbitrary units). From Eqs. A3 and A4, $\bar{V} \approx -40$ mV and $V_{1/2} \approx 42$ mV. (A) Symbols, simulated $t_d(V)$ and $S_{Max}(V)$. Thick lines, predicted delay or maximum slope without deactivation. Deactivation shortens the delay and reduces the maximum slope for all but the highest voltages. Thin line (delay), fit of $t_d(V)$ with the four-step model (Eq. 4), apparent $\alpha_0 = 1.7$ and $z_\alpha = 0.66$. Thin line (slope), fit of $S_{max}(V)$ with Eq. 3 and z_α forced to the value from the delay fit. The resulting fit is not very good, $S_{max}(V)$ is somewhat steeper. (Inset) Experimental example. $t_d(V)$ and $S_{Max}(V)$ relations (delay fit, $\alpha_0 = 6.7\ s^{-1}$, $z_\alpha = 0.57$; slope fit, z_α forced to 0.57). (B) Fits of simulated P_O(t) rise (thick lines) with Eq. 2 and the apparent parameters from the $t_d(V)$ fit (thin lines). At 0 mV, the fit amplitude is larger, and at 30 mV it is smaller than the peak P_O. At 90 mV, Eq. 2 needs to be strongly upscaled to fit the early rising phase of P_O. (Inset) Experimental example, as in A. When fitting the recorded current rise with Eq. 2 and the parameters from the delay fit, the fit amplitudes at 0 and 30 mV are smaller, and at 90 mV larger than the peak current.

too slow and the Eq. 2 fit must be upscaled to match the simulated rise.

The insets in Fig. 11, A and B, show one of the 2 (of 13) datasets that behaved similarly. $S_{Max}(V)$ is not quite adequately described by z_α from the $t_d(V)$ fit, and fits of the current rise at 0 and 30 mV with Eq. 2 and the parameters from the $t_d(V)$ fit undershoot the peak experimental currents. Both features are reminiscent of the simulation results and could be interpreted as pointing toward deactivation with $z_\beta < z_\alpha$. In this regime, our estimates of z_α and α_0 would be affected by deactivation.

Overall, our data revealed only a few hints of deactivation influence, reconfirming that deactivation can be neglected for most voltages. However, some experimental findings could be explained by deactivation with $z_\beta \leq z_\alpha$ (Fig. 11)—in this kinetic regime, deactivation affects channel activation if β_0 is high enough. The signature behavior was observed in a minority of experiments, perhaps reflecting sensitivities of activation and deactivation steps to biotic factors that varied among oocytes. Changes in β_0 also shift $V_{1/2}$ and $\bar{V}$ (see Eqs. A3 and A4). Our 5aa data thus seem most consistent with $z_\beta \leq z_\alpha$, since a bend in the $t_d(V)$ relation may also occur in this regime (see Fig. 11 A).

3. Concerted Last Activation Steps

Final concerted activation steps would be pore-opening transitions happening simultaneously in all subunits after the voltage sensors moved. If voltage sensor and pore-opening movements are separate, there is no immediate "need" for the pore opening to be voltage sensitive, but it might still be. For the Shaker ILT mutant, the pore opening step is rate limiting and slightly voltage-dependent (Ledwell and Aldrich, 1999). For WT, the last step in the activation sequence is reported to be voltage insensitive (Rodriguez and Bezanilla, 1996). WT may have multiple concerted transitions (Schoppa and Sigworth, 1998c propose two) whose kinetic significance varies among mutants. To assess whether a final concerted step plays a role for 5aa activation kinetics, we considered the impact of such a step on our ability to fit simulated $t_d(V)$, $S_{Max}(V)$ and P_O(t) using Scheme I (Eqs. 2–4).

A voltage-insensitive last step cannot be rate limiting in 5aa at all voltages. The rate-limiting step determines the maximum slope, while nonlimiting steps contribute only to the delay: S^P_{Max} would be voltage independent and S_{Max} would show only the (linear) voltage dependence of the driving force. Instead, $S_{Max}(V)$ was usually well described (e.g., Figs. 4 and 6) by the product of a linear and an exponential term. Moreover, with one rate-limiting step, the current rise would be monoexponential, hardly resembling the fourth order exponential in Eq. 2.

Likewise, we can dismiss a voltage-independent last step with intermediate rate faster than $\alpha(V)$ at small voltages, but rate limiting with increasing $\alpha(V)$ at high depolarizations. This would make $S^P_{Max}(V)$ exponential at low V, till it approached some constant value at high V, with $S_{Max}(V)$ becoming linear accordingly. We never encountered this in 5aa data and can thus exclude the possibility that 5aa activation kinetics were shaped by voltage-independent concerted steps. (A fast voltage-independent concerted step would not affect channel activation kinetics at all.)

What about voltage-dependent concerted steps? If the final step were rate-limiting at some or all voltages, Eq. 2 would not describe the P_O(t) rise. The only scenario the analysis cannot exclude is a final concerted step with voltage-dependent rate similar in both basic

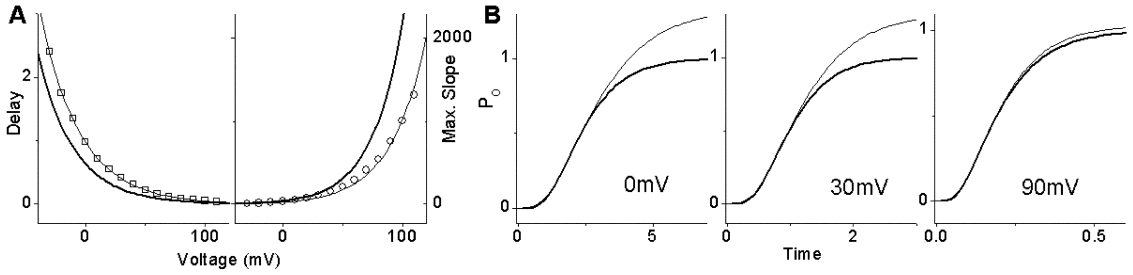

FIGURE 12. Simulated kinetic data for four irreversible subunit activation steps and one final concerted transition with rate $c = c_0 e^{z_c 0.039\,V}$. $\alpha_0 = 1$, $z_\alpha = 0.85$, $\gamma_0 = 2$, $z_\gamma = 0.42$ (arbitrary units). (A) Symbols, simulated $t_d(V)$ and $S_{Max}(V)$. Thick lines, predicted delay or maximum slope without (i.e., with infinitely fast) last step. Naturally, the additional step prolongs the delay and slows the current rise. Thin line (delay), fit of $t_d(V)$ with Eq. 4, apparent $\alpha_0 = 0.65$ and $z_\alpha = 0.9$. Thin line (slope), fit of $S_{Max}(V)$ with Eq. 3, z_α forced to the value from the delay fit. $S_{Max}(V)$ is really somewhat biphasic, but can be described satisfyingly with $z_\alpha = 0.9$. (B) Simulated P_O(t) (thick lines) and fits with Eq. 2, α_0 and z_α from the delay fit (thin lines). The fits look reasonable at all voltages. Upscaling of the fit expression is required, but if we encountered this effect in our experiments, we couldn't easily differentiate it from that of inactivation.

rate and gating charge to the subunit activation rate. Fig. 12 shows simulations for an example with four irreversible subunit activation steps and a final concerted step with rate $\gamma(V)$ that has a somewhat shallower voltage dependence than $\alpha(V)$. At small V, $\gamma(V)$ is slightly faster, at large V it is slower than $\alpha(V)$. The simulated $t_d(V)$ in the of Fig. 12 A, left, is larger than the corresponding delay for the simple four-step model, as expected for one additional activation step. $t_d(V)$ is well fitted by the four-step model, with underestimated $\alpha(V)$. S_{Max} shows a very slight biphasicity—at small V, it is dominated by $\alpha(V)$, while at large V, $\gamma(V)$ and its shallower voltage dependence dominate. However, the four-step model and z_α from the $t_d(V)$ fit describe $S_{Max}(V)$ adequately. Simulated P_O(t) in Fig. 12 B all saturate at unity, since we neglected inactivation and deactivation to isolate the effect of the concerted step. The P_O(t) rise can be described by Eq. 2 and the apparent α_0 and z_α from the delay fit, but Eq. 2 must be upscaled to match the simulated rise—the final amplitudes of all fits exceed one. In this example, less upscaling of Eq. 2 is required at large voltages. If $\gamma(V)$ and $\alpha(V)$ are identical, the scaling factor is the same at all voltages (simulations not shown).

Thus, besides inactivation, an additional voltage-dependent concerted activation step might contribute to the often encountered mismatch of current and fit amplitudes (like Fig. 9 C).

4. Two Activation Steps per Subunit

The Shaker WT voltage sensor may move in two or three kinetically distinguishable steps (e.g., Schoppa and Sigworth, 1998c) and there is no reason to think steps vanish in 5aa. Since 5aa activation kinetics seem quite well explained by one rate-limiting step per subunit, might we be describing the kinetic properties of eight-step activation by a four-step model with apparent parameters?

Model simulations with two subunit activation steps suggest not, since they do not produce behavior that could be mistaken for a four-step scheme. For two steps with similar or identical gating charges, $t_d(V)$ and $S_{max}(V)$ are well described by the four-step model (Fig. 13 A), but the apparent α_0 from the delay fit is far smaller than the basic rates of the two activation steps. Thus, Eq. 2 must be upscaled to match the simulated P_O rise—the amplitude mismatch between simulation and fit is large at all voltages. More characteristically, even though the delays t_d of the eight-step simulation and the four-step Eq. 2 with apparent parameters are identical, the sigmoidicity of the eight-step P_O(t) is not seen with four-step (Fig. 13 B). This pattern was never encountered in fitting 5aa currents with Eq. 2, so we conclude that 5aa does not have two kinetically significant subunit activation steps with identical or similar gating charges.

If the two steps have different gating charges, the smaller charge always gains significance in model behavior at large V, e.g., system kinetics may go from eight-step to effectively four-step. Thus, the smaller charge has disproportionately large influence on $S_{Max}(V)$, making it impossible to describe the steepness of $t_d(V)$ and $S_{Max}(V)$ by the same exponent. P_O(t) for such a system cannot be described by Eq. 2 and the parameters from the $t_d(V)$ fit. An example demonstrates. Fig. 13, C and D, shows simulated eight-step data for equal basic rates, but different activation step gating charges (0.85 and 1.35). The $t_d(V)$ relation (Fig. 13 C, left) is more influenced by the model properties at small V, where delays are long, while $S_{Max}(V)$ (right panel) is dominated by the steep slopes at large V. There, model kinetics approximate those of a four-step model dominated by the slower of the two rates. Consequently, $S_{Max}(V)$ is well fitted by the four-step model with $z_\alpha = 1$ (thick line). The $t_d(V)$ fit with Eq. 4 produces an apparent $z_\alpha = 1.2$ (thin line) (a sort of weighted aver-

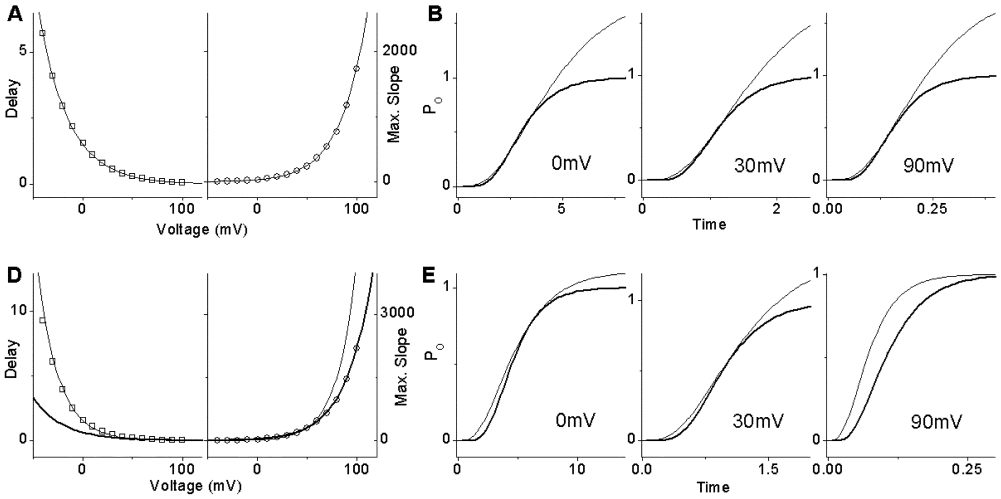

FIGURE 13. Simulated kinetic data for two irreversible subunit activation steps. (A and B) Similar rates at all voltages. $\alpha_{10} = 1$, $\alpha_{20} = 1.2$, $z_{\alpha 1} = 0.85$, $z_{\alpha 2} = 0.85$ (arbitrary units). (A) Symbols, simulated $t_d(V)$ and $S_{max}(V)$. Thin line (delay), fit with the four-step model (Eq. 4), apparent $\alpha_0 = 0.42$ and $z_\alpha = 0.85$. Thin line (slope), fit with Eq. 3 and z_α from the delay fit. (B) Simulated P_O(t) (thick lines) and fits with Eq. 2, α_0 and z_α from the delay fit (thin lines). Upscaling of the fit expression is required for all voltages to reproduce the simulated maximum slope. The fitted curves from the four-step model are less sigmoidal. (C and D) Different rates (one is rate-limiting at high voltages). $\alpha_{10} = 1$, $\alpha_{20} = 1$, $z_{\alpha 1} = 0.85$, $z_{\alpha 2} = 1.35$ (arbitrary units). (C) Symbols, simulated $t_d(V)$ and $S_{Max}(V)$. Thin line (delay), fit of $t_d(V)$ with Eq. 4, apparent $\alpha_0 = 0.4$ and $z_\alpha = 1.2$. Thick line (delay), Eq. 4 with $\alpha_0 = 1$ and $z_\alpha = 0.85$, the parameters that fit $S_{Max}(V)$. Thin line (slope), trying to describe S_{Max} with Eq. 3 and z_α from the delay fit. Thick line (slope), Eq. 3 with $\alpha_0 = 1$ and $z_\alpha = 0.85$ describes $S_{Max}(V)$ well. (B) Simulated P_O(t) (thick lines) and fits with Eq. 2, α_0 and z_α from the delay fit (thin lines). At small voltages, the maximum slope can be reproduced by upscaling Eq. 2, but the eight-step P_O(t) is always more sigmoidal. At large voltages (e.g., 90 mV), P_O(t) rises more slowly than Eq. 2 as the step with $\alpha_{10} = 1$ and $z_{\alpha 1} = 0.85$ becomes rate limiting: at 90 mV, it is threefold slower than the rate predicted from the delay fit.

age of the two gating charges), together with a vastly underestimated apparent $\alpha_0 = 0.4$ (a much slower rate is needed to produce the same t_d value in the four-step model as two faster rates in the 8-step model). Fig. 13 D shows simulated P_O(t), which are not described by Eq. 2 with the apparent parameters from the $t_d(V)$ fit. First, the 4-step model cannot reproduce the combination of long eight-step delays plus relatively big S_{Max} at small V. Second, even though the model is effectively four-step at large V, the limiting rate ($\alpha_0 = 1$, $z_\alpha = 0.85$) is smaller than predicted from the $t_d(V)$ fit.

In this eight-step activation example, neither $t_d(V)$ and $S_{Max}(V)$ nor P_O(t) come close to being described by a four-step model. This should be true whenever the two subunit activation steps have different gating charges, whether they start with similar or different rates at low V, thus also ruling out two subunit activation steps with different gating charges as a candidate for the 5aa activation model.

APPENDIX B

Influence of Activation and Inactivation Rates on Current Decline

If $i >> \alpha$ (the case of rate-limiting activation), we may employ a quasi-steady-state approximation for O on the time scale $t' = \alpha\, t$ of the changes in C_0 to C_3.

$$\frac{dO}{dt} = \alpha \cdot C_3 - i \cdot O$$

$$0 \approx \frac{\alpha}{i}\frac{dO}{dt'} = \frac{\alpha}{i} \cdot C_3 - O.$$

In that case, the time course of O is a scaled version of C_3(t), $0 \approx \frac{\alpha}{i} C_3$. If all channels are initially in the left-most closed state of Scheme II ($P_{C_0}(t = 0) = 1$), the P_O time course is

$$P_O(t)|_{i \ll \alpha} \approx \frac{\alpha}{i}(-4e^{-4\alpha t} + 12e^{-3\alpha t} - 12e^{-2\alpha t} + 4e^{-\alpha t}). \quad \text{(A6)}$$

The inactivation rate i is irrelevant for falling phase kinetics (instead the P_O decline might be approximated as the sum of two exponentials with the two slowest rates, 2α and α), and the voltage sensitivity of the decline rate comes from $\alpha(V)$. In fact, voltage will have the same effect on both current rise and decline: P_O time courses at all voltages are identical if time and amplitude are scaled by α (in case of the amplitude, really by α/i, but i was assumed constant for now). Note that this sort of rate limitation ($i >> \alpha$) excludes P_O saturation—the P_O(t) amplitudes in Eq. A6 are tiny.

If $i \cong \alpha$, the quasi-steady-state approximation fails and a fifth exponential term with rate i enters the expression for P_O(t),

$$P_O(t)|_{i \cong \alpha} = a_1 e^{-4\alpha t} + a_2 e^{-3\alpha t} + a_3 e^{-2(4)\alpha t} + a_4 e^{-\alpha t} - (a_1 + a_2 + a_3 + a_4) e^{-it}. \quad \text{(A7)}$$

The coefficients a_1 to a_4 are simple functions of α and i (e.g., $a_1 = \frac{4\alpha}{4\alpha - i}$), but we don't profit from resolving them here.

If $i << \alpha$ (as for WT), $e^{-it} \approx 1$ on the time scale of the fast changes governed by α and its multiples. Further, the coefficients a_1 to a_4 in Eq. A2 simplify, resulting in

Eq. 2 for the P_O rise and a simple exponential P_O decline with rate *i*. In this regime, without deactivation, peak P_O is always 1.

We thank Dr. Peter Juranka for technical assistance, and Dr. Richard Horn for a helpful discussion of the manuscript.

This work was supported by operating grants to C.E. Morris from NSERC, Canada and the Canadian Institutes of Health Research.

Olaf S. Andersen served as editor.

Submitted: 20 October 2003
Accepted: 29 December 2003

REFERENCES

Aggarwal, S.K., and R. MacKinnon. 1996. Contribution of the S4 segment to gating charge in the Shaker K^+ channel. *Neuron.* 16: 1169–1177.

Bezanilla, F. 2000. The voltage sensor in voltage-dependent ion channels. *Physiol. Rev.* 80:555–592.

Bezanilla, F. 2002. Voltage sensor movements. *J. Gen. Physiol.* 120: 465–473.

Blount, P. 2003. Molecular mechanisms of mechanosensation: big lessons from small cells. *Neuron.* 37:731–734.

Broomand, A., R. Männikkö, H.P. Larsson, and F. Elinder. 2003. Molecular movement of the voltage sensor in a K channel. *J. Gen. Physiol.* 122:741–748.

Calabrese, B., I.V. Tabarean, P. Juranka, and C.E. Morris. 2002. Mechanosensitivity of N-type calcium channel currents. *Biophys. J.* 83:2560–2574.

Cha, A., G.E. Snyder, P.R. Selvin, and F. Bezanilla. 1999. Atomic scale movement of the voltage-sensing region in a potassium channel measured via spectroscopy. *Nature.* 402:809–813.

Conti, F., R. Fioravanti, J.R. Segal, and W. Stuehmer. 1982. Pressure dependence of the sodium currents of squid giant axon. *J. Membr. Biol.* 69:23–34.

Gandhi, C.S., and E.Y. Isacoff. 2002. Molecular models of voltage sensing. *J. Gen. Physiol.* 120:455–463.

Gandhi, C.S., E. Clark, E. Loots, A. Pralle, and E.Y. Isacoff. 2003. The orientation and molecular movement of a K^+ channel voltage-sensing domain. *Neuron.* 40:515–525.

Gauss, R., R. Seifert, and U.B. Kaupp. 1998. Molecular identification of a hyperpolarization-activated channel in sea urchin sperm. *Nature.* 393:583–591.

Glauner, K.S., L.M. Mannuzzu, C.S. Gandhi, and E.Y. Isacoff. 1999. Spectroscopic mapping of voltage sensor movement in the Shaker potassium channel. *Nature.* 402:813–817.

Gonzalez, C., E. Rosenman, F. Bezanilla, O. Alvarez, and R. Latorre. 2001. Periodic perturbations in Shaker K^+ channel gating kinetics by deletions in the S3-S4 linker. *Proc. Natl. Acad. Sci. USA.* 98: 9617–9623.

Gonzalez, C., E. Rosenman, F. Bezanilla, O. Alvarez, and R. Latorre. 2000. Modulation of the Shaker K^+ channel gating kinetics by the S3-S4 linker. *J. Gen. Physiol.* 115:193–208.

Goodman, M.B., and E.M. Schwarz. 2003. Transducing touch in *Caenorhabditis elegans. Annu. Rev. Physiol.* 65:429–452.

Gu, C., P.F. Juranka, and C.E. Morris. 2001. Stretch activation and inactivation of Shaker-IR, a voltage-gated K^+ channel. *Biophys. J.* 80:2678–2693.

Hajdu, P., Z. Varga, C. Pieri, G. Panyi, and R. Gaspar, Jr. 2003. Cholesterol modifies the gating of Kv1.3 in human T lymphocytes. *Pflugers Arch.* 445:674–682.

Hille, B. 2001. Ion Channels of Excitable Membranes. 3rd edition. Sinauer Associates Inc., Sunderland, MA. 622 pp.

Horn, R. 2002. Coupled movements in voltage-gated ion channels. *J. Gen. Physiol.* 120:449–453.

Hoshi T., W.N. Zagotta, and R.W. Aldrich. 1990. Biophysical and molecular mechanisms of Shaker potassium channel inactivation. *Science.* 250:533–538.

Hoshi, T., W.N. Zagotta, and R.W. Aldrich. 1994. Shaker potassium channel gating. I: Transitions near the open state. *J. Gen. Physiol.* 103:249–278.

Jiang, Y., A. Lee, J. Chen, V. Ruta, M. Cadene, B.T. Chait, and R. MacKinnon. 2003a. X-ray structure of a voltage-dependent K+ channel. *Nature.* 423:33–41.

Jiang, Y., V. Ruta, J. Chen, A. Lee, and R. MacKinnon. 2003b. The principle of gating charge movement in a voltage-dependent K+ channel. *Nature.* 423:42–48.

Klemic, K.G., G.E. Kirsch, and S.W. Jones. 2001. U-type inactivation of Kv3.1 and Shaker potassium channels. *Biophys. J.* 81:814–826.

Langton, P.D. 1993. Calcium channel currents recorded from isolated myocytes of rat basilar artery are stretch sensitive. *J. Physiol.* 471:1–11.

Larsson, H.P., O.S. Baker, D.S. Dhillon, and E.Y. Isacoff. 1996. Transmembrane movement of the shaker K+ channel S4. *Neuron.* 16:387–397.

Ledwell, J.L., and R.W. Aldrich. 1999. Mutations in the S4 region isolate the final voltage-dependent cooperative step in potassium channel activation. *J. Gen. Physiol.* 113:389–414.

Loots, E., and E.Y. Isacoff. 2000. Molecular coupling of S4 to a K(+) channel's slow inactivation gate. *J. Gen. Physiol.* 116:623–636.

Lopez-Barneo, J., T. Hoshi, S.H. Heinemann, and R.W. Aldrich. 1993. Effects of external cations and mutations in the pore region on C-type inactivation of Shaker potassium channels. *Receptors Channels.* 1:61–71.

Macdonald, A.G. 2002. Experiments on ion channels at high pressure. *Biochim. Biophys. Acta.* 1595:387–389.

Mienville, J., J.L. Barker, and G.D. Lange. 1996. Mechanosensitive properties of BK channels from embryonic rat neuroepithelium. *J. Membr. Biol.* 153:211–216.

Meyer, R., and S.H. Heinemann. 1997. Temperature and pressure dependence of Shaker K^+ channel N- and C-type inactivation. *Eur. Biophys. J.* 26:433–445.

Naruse, K. Q. Tang, Q. Zhi, and M. Sokabe. 2003. Cloning and functional expression of a stretch-activated BK channel (SAKCa) from chick embryonic cardiomyocyte. *Biophys. J.* 83:234A.

Olcese, R., R. Latorre, L. Toro, F. Bezanilla, and E. Stefani. 1997. Correlation between charge movement and ionic current during slow inactivation in Shaker K^+ channels. *J. Gen. Physiol.* 110:579–589.

Ordway, R.W., S. Petrou, M.T. Kirber, J.V. Walsh Jr., and J.J. Singer. 1995. Stretch activation of a toad smooth muscle K^+ channel may be mediated by fatty acids. *J. Physiol.* 484:331–337.

Ou, Y., P. Strege, S.M. Miller, J. Makielski, M. Ackerman, S.J. Gibbons, and G. Farrugia. 2003. Syntrophin gamma 2 regulates SCN5A gating by a PDZ domain-mediated interaction. *J. Biol. Chem.* 278:1915–1923.

Pahapill, P.A., and L.C. Schlichter. 1992. Modulation of potassium channels in intact human T lymphocytes. *J. Physiol.* 445:407–430.

Ren, D., B. Navarro, G. Perez, A.C. Jackson, S. Hsu, Q. Shi, J.L. Tilly, and D.E. Clapham. 2001a. A sperm ion channel required for sperm motility and male fertility. *Nature.* 413:603–609.

Ren, D., B. Navarro, H. Xu, L. Yue, Q. Shi, and D.E. Clapham. 2001b. A prokaryotic voltage-gated sodium channel. *Science.* 294: 2372–2375.

Rodriguez, B.M., and F. Bezanilla. 1996. Transitions near the open state in Shaker K^+-channel: probing with temperature. *Neuropharmacology.* 35:775–785.

Scarlata, S.F. 1991. Effect of increased chain packing on gramicidin-lipid interactions. *Biochemistry.* 30:9853–9859.

Schoenmakers, T.J., H. Vaudry, and L. Cazin. 1995. Osmo- and mechanosensitivity of the transient outward K^+ current in a mammalian neuronal cell line. *J. Physiol.* 489:419–440.

Schoppa, N.E., K. McCormack, M.A. Tanouye, and F.J. Sigworth. 1992. The size of gating charge in wild-type and mutant Shaker potassium channels. *Science.* 255:1712–1715.

Schoppa, N.E., and F.J. Sigworth. 1998a. Activation of shaker potassium channels. I. Characterization of voltage-dependent transitions. *J. Gen. Physiol.* 111:271–294.

Schoppa, N.E., and F.J. Sigworth. 1998b. Activation of Shaker potassium channels. II. Kinetics of the V2 mutant channel. *J. Gen. Physiol.* 111:295–311.

Schoppa, N.E., and F.J. Sigworth. 1998c. Activation of shaker potassium channels. III. An activation gating model for wild-type and V2 mutant channels. *J. Gen. Physiol.* 111:313–342.

Seoh, S.A., D. Sigg, D.M. Papazian, and F. Bezanilla. 1996. Voltage-sensing residues in the S2 and S4 segments of the Shaker K^+ channel. *Neuron.* 16:1159–1167.

Shcherbatko, A., F. Ono, G. Mandel, and P. Brehm. 1999. Voltage-dependent sodium channel function is regulated through membrane mechanics. *Biophys. J.* 77:1945–1959.

Smith-Maxwell, C.J., J.L. Ledwell, and R.W. Aldrich. 1998. Role of the S4 in cooperativity of voltage-dependent potassium channel activation. *J. Gen. Physiol.* 111:399–420.

Starkus, J.G., L. Kuschel, M.D. Rayner, and S.H. Heinemann. 1997. Ion conduction through C-type inactivated Shaker channels. *J. Gen. Physiol.* 110:539–550.

Starkus, J.G., S.H. Heinemann, and M.D. Rayner. 2000. Voltage dependence of slow inactivation in Shaker potassium channels results from changes in relative K^+ and Na^+ permeabilities. *J. Gen. Physiol.*115:107–122.

Tabarean, I.V., and C.E. Morris. 2002. Membrane stretch accelerates activation and slow inactivation in Shaker channels with S3-S4 linker deletions. *Biophys. J.* 82:2982–2994.

Tabarean, I.V., P. Juranka, and C.E. Morris. 1999. Membrane stretch affects gating modes of a skeletal muscle sodium channel. *Biophys. J.* 77:758–774.

Taniguchi, J., and W.B. Guggino. 1989. Membrane stretch: a physiological stimulator of Ca^{2+}-activated K^+ channels in thick ascending limb. *Am. J. Physiol.* 257:F347–F352.

Yang, X.C., and F. Sachs. 1989. Block of stretch-activated ion channels in *Xenopus* oocytes by gadolinium and calcium ions. *Science.* 243:1068–1071.

Yellen, G. 2002. The voltage-gated potassium channels and their relatives. *Nature* 419:35–42.

Yifrach, O., and R. MacKinnon. 2002. Energetics of pore opening in a voltage-gated K(+) channel. *Cell.* 111:231–239.

Yusaf, S.P., D. Wray, and A. Sivaprasadarao. 1996. Measurement of the movement of the S4 segment during the activation of a voltage-gated potassium channel. *Pflugers Arch.* 433:91–97.

Zagotta, W.N., T. Hoshi, J. Dittman, and R.W. Aldrich. 1994a. Shaker potassium channel gating. II: Transitions in the activation pathway. *J. Gen. Physiol.* 103:279–319.

Zagotta, W.N., T. Hoshi, and R.W. Aldrich. 1994b. Shaker potassium channel gating. III: Evaluation of kinetic models for activation. *J. Gen. Physiol.* 103:321–362.